OPTIMIZATION OF SILK PROCESSING FOR ENHANCED MECHANICAL PROPERTIES

A thesis

submitted by

Benjamin P. Partlow

In partial fulfillment of the requirements
for the degree of

Masters of Science

in

Mechanical Engineering

TUFTS UNIVERSITY

August, 2012

Adviser: Gary Leisk

Abstract

Native silk fibers have been exploited in clinical applications for replacing and strengthening connective tissues including ligaments and tendons and in the closure of wounds. However, more recent work has focused on the use of reconstituted silk to create three dimensional tissue scaffolds that can be used to regenerate living tissue replacements. This work takes advantage of the fact that silk fibroin is a naturally occurring, biocompatible polymer and can be formed into myriad constructs including fibers, films, foams and sponges. While this has opened up numerous new opportunities for the use of silk in biomedical engineering one of the major hurdles has been achieving mechanical properties as robust as those exhibited by natural silk fibroin in a regenerated form. This work explores the effect of the reconstitution process on the quality of the regenerated silk solution and solid constructs through molecular weight, rheological and mechanical analysis. These tests have also provided insight into the self assembly process enabling the optimization of mechanical properties.

Acknowledgements

I would like to acknowledge and thank my professors Gary Leisk and David Kaplan for introducing me to the fields of biopolymers and tissue engineering and for their support throughout this project. In addition I would like to thank Prof. Luisa Chiesa for serving on my thesis committee, Tim Lo, for teaching me the processes involved in reconstituting silk and assistance in the lab and Jon Kluge for philosophizing about the mechanisms involved in the silk processing. Finally I would to thank friends and family for their support and interest in this research project.

Table of Contents

List of Figures

List of Tables

OPTIMIZATION OF SILK PROCESSING FOR ENHANCED MECHANICAL PROPERTIES

1. Introduction

Silk from the domesticated silkworm, *Bombyx mori*, is an extremely tough and versatile material that has been used as a cloth for millennia, sutures for centuries and more recently in a regenerated form as scaffolds for tissue engineering [1-4], sustained drug delivery [5-7] and technological applications [8-10]. This diverse array of applications stems from the exploitation of silks highly evolved protein structure and the silkworms sophisticated processing mechanisms which imbue the fiber with exceptional strength and extensibility [11]. The amino acid sequence of the primary structural component of the silk protein, fibroin, when processed properly, allows for close packing and highly aligned molecules, giving silk its amazing mechanical properties. The combination of high tensile strength, excellent ductility and extreme toughness rivals those of synthetic fibers [12].

While use of the silk in its native fiber form has been exploited in biomedical engineering for use in replacing and strengthening primarily connective tissues including ligaments and tendons and in the closure of wounds, current work has focused on the use of silk solutions that have been dissolved and reconstituted to create three dimensional tissue scaffolds. The advantage of this approach is that the silk fibroin is a naturally occurring biocompatible polymer and can be formed into myriad constructs including fibers, films, foams and sponges. These constructs also allow incorporation of various drugs or growth factors to ensure healthy tissue growth and can be tuned to degrade over specified time periods [13].

Table 1 indicates some of the applications of silk in biomedical engineering and the preferred morphology. Films are primarily used where a covering is of primary importance and strength is of secondary concern, as in wound dressings and the prevention of thrombogenesis. Sponges and hydrogels, which are highly porous 3-d constructs are used where filling of voids is required, such as soft tissue and major bone defect regeneration. Fibers and non-woven (electrospun) mats are used where restoration of mechanical strength are necessary for the success of the intervention, including ligament, tendon and connective tissue repairs.

Table 1 - Cell and tissue applications of silk fibroin scaffolds. From Vepari and Kaplan 2007 [13].

Application	Morphology	References
Wound dressings	Film	[14]
	Sponge	[15]
Bone tissue engineering	Sponge	[16-22]
	Film	[23-25]
	Hydrogel	[26, 27]
	Non-woven	[28, 29]
Cartilage tissue engineering	Porous sponge	[22, 30-33]
	Hydrogel	[34]
Ligament tissue engineering	Fiber	[35-37]
Tendon tissue engineering	Fibers	[38]
Hepatic tissue engineering	Films	[39]
Connective tissue	Non-woven mats	[40]
Endothelial and blood vessel	Non-woven mats	[41, 42]
Antithrombogenesis	Films	[43]

While regenerated silk constructs have been shown to be an intriguing material for use in biomedical engineering, their mechanical properties are significantly weaker than those exhibited by native silk fibers. There have been a number of potential explanations for the inability to regenerate fibers with mechanical properties comparable to those of native fibers, including protein degradation during solubilization [44] and improper alignment of the molecules and self assembled nanofibrils [45].

In order to elucidate the impact of the silk solubilization conditions on the mechanical properties of regenerated silk fibroin constructs, a series of experiments were undertaken in order to minimize protein degradation during processing. These silk solutions were then subjected to a battery of testing in the solution state (gel electrophoresis, viscometry and rheometry) and in the solid film state (steam drawing, tensile testing and fourier transform infrared spectroscopy (FTIR)). These test conditions allowed for the determination of important parameters that affect regenerated fibroins material properties and suggest optimized processing conditions to achieve enhanced mechanical properties.

2. Background

2.1. Silk Chemistry and Structure

Native silk fibers, as spun by the domesticated *Bombyx mori* silkworm, are formed from two proteins, fibroin and sericin in an approximate mass ratio of 70-80% to 20-30% respectively with 1-2% residual contaminants including waxes and ash. The fibroin is further subdivided into heavy and light chains and no fewer than three distinct types of sericin have been reported. As depicted in Figure 1, the sericin is a glue like protein that coats an inner core consisting of two filaments or brins of fibroin. These brins are made up of fibrils and microfibrils. Each fibril is on the order of 1µm in diameter and is composed of approximately 1,000 microfibrils with diameters of 100-150 Å. The microfibrils consist of micelles composed solely of the protein fibroin and carefully assembled into crystalline and amorphous segments [46].

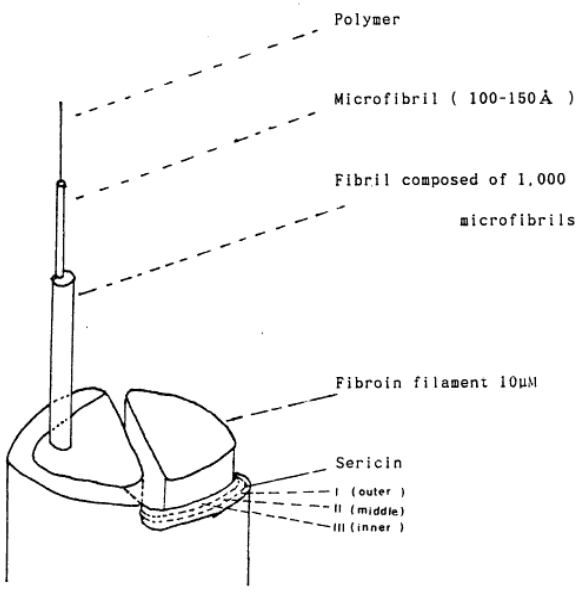

Figure 1 - Structural architecture of a silk fiber, indicating two fibroin brins, or filaments, with sericin coating. Adapted from Silk Reeling and Testing Manual [46].

These crystalline and amorphous regions of the micelles arise from highly repetitive amino acid sequences comprising the heavy chain fibroin. The fibroin chain is comprised of 12 highly order crystalline domains Gly – X repeats, which account for 94% of the chain length. In the sequence "X" is replaced by alanine in 65%, serine in 23% and tyrosine in 9% of the structural repeats. These repeats, composed primarily of hydrophobic amino acids, allow for the assembly of the (Gly-Ala-Gly-Ala-Gly-Ser) repeat segments in anti-parallel β-sheets. The anti-parallel configuration is shown schematically in Figure 2 where the sequence is from left-to-right in the top and bottom layers and right-to-left in the middle. The remainder of the sequence consists of 11 hydrophilic linkers between the crystalline domains and N-terminal and C-terminal sequences that are similarly hydrophilic [47].

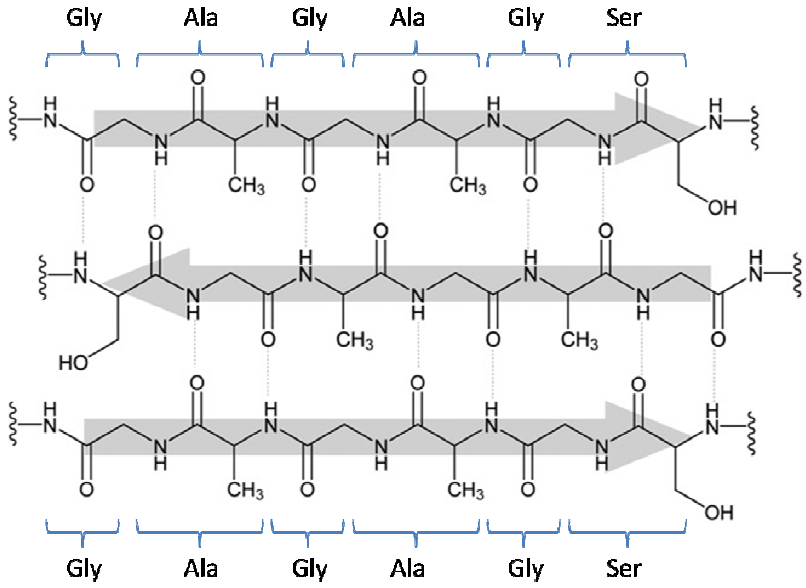

Figure 2 - Schematic of anti-parallel β-sheet formation in (Gly-Ala-Gly-Ala-Gly-Ser) repeat sequence of silk fibroin. Adapted from Murphy and Kaplan, 2009 [48].

This protein sequence of alternating hydrophilic and hydrophobic blocks has been shown to cause the formation of micelles in aqueous solutions, as depicted in Figure 3. The intra and inter-molecular hydrophobic-hydrophilic interactions result in self organization where the polar N and C-terminals migrate toward the outside while the hydrophobic crystalline domains fold on themselves and are sequestered in the center of the micelle. As multiple fibroin chains agglomerate the micelle grows to a critical size and additional micelles form and associate with each other to form fibroin globules. Then, when the silkworm spins fibers the globules are subjected to elongational shear, taking on an oblong shape and creating the multi-level fibrillar structure [49].

This ordered self assembly of the silk fibroin molecules allows for the generation of a highly crystalline biopolymer, with robust mechanical properties. In addition, the elimination of water from the hydrophobic core of the micelles allows for rapid evaporation of the water solvent/plasticizer upon extrusion from the silk gland. This allows the *B. mori* silkworm to rapidly spin fibers under ambient conditions without the use of highly volatile solvents that are typically used in synthetic polymer manufacture [50].

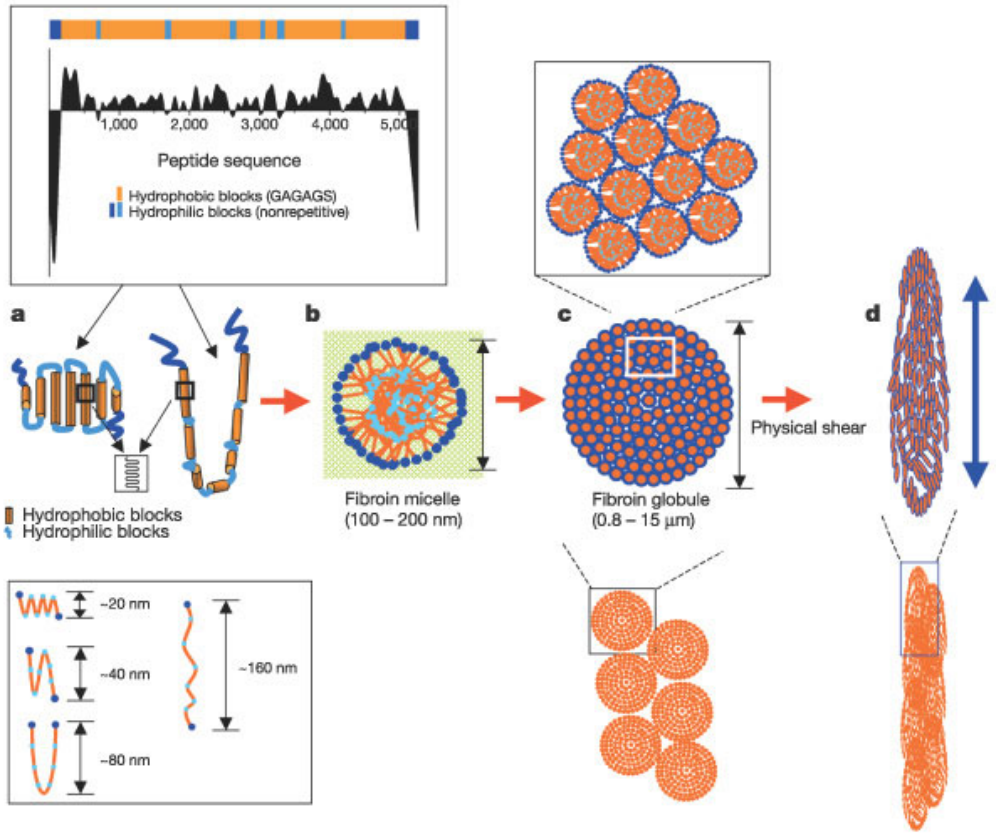

Figure 3 - Schematic of chain folding, micelle formation, globule formation and shear of silk protein. a, Hydrophobicity pattern in fibroin heavy chain. b, Chain folding and micelle formation. c, Globule formation driven by increase in silk concentration. d, Shear and alignment in spinning.

The molecular weights of the native silk fibroin heavy and light chains, extracted from the *B. mori* pupae, are 370 and 25 kDa respectively. These two chains occur in equal proportions and are connected at their C-terminus by a disulfide linkage [51-53]. The sericins are similarly large proteins with molecular weights on the order of 400 kDa [54]. Due to its implication in inflammatory responses, the sericin protein is removed from the raw silk in a process known as degumming, leaving pure silk fibroin for use in any application where there is exposure to cells [1]. While there are multiple ways to remove the sericin, one of the most commonly employed degumming processes involves submerging the

cocoons in a heated bath with a 0.02 molar concentration of sodium carbonate (Na_2CO_3) at approximately 98 ^oC (boiling point) for 20-30 minutes [55]. This process serves to break apart the compacted cocoon fibers and remove the hydrophilic sericin compounds leaving pure fibroin protein fibers.

While the extraction of sericin proteins from the fibers is necessary to avoid inflammatory responses *in vivo* [56, 57], this process also results in the degradation, or shortening, of the protein chains. Most of the literature on regenerated silk fibroin to date has utilized silk that has been degummed for 20-30 minutes or longer. This degree of degumming results in protein degradation from an average molecular weight of 370 kDa and polydispersity of nearly 1 (homogenous with all chains of equal length) to a broad distribution of weights from undegraded strands of 370 kDa to small fragments of 40-50 kDa and a number average molecular weight on the order of 150 kDa [58]. This significant degradation of the protein chain is a necessary step for effective use of silks in biomedical engineering, however, its impact on the nature of the self assembly process and thereby mechanical properties are incompletely understood.

2.2. Previous Work

Due to its promising nature in the field of biomedical and tissue engineering there is a substantial body of literature devoted to the understanding of silk fibroin and its interaction with cells and tissues. A search of PubMed, under the term "silk fibroin", returns nearly 1,400 scholarly articles on the subject, with 65% of these being published within the last 10 years. A review of this literature is included below with an emphasis on works dedicated to the understanding and optimization of the self assembly mechanisms of the fibroin chains and enhancing the mechanical properties of the silk.

2.2.1. Optimizing Fiber Degumming

Given silks long history of use as a fabric and its economic importance, the reeling and degumming processes have been heavily studied and optimized to efficiently produce consistent fibers of the highest quality. While these studies do not directly apply to the use of regenerated silks, it can be presumed that the same mechanisms that degrade the sheen and tenacity of degummed native fibers will have similar deleterious effects on silks that have been regenerated.

Jiang et al. directly compared the impact on the mechanical behavior of silk fibers that were degummed using different chemical agents that are commonly reported in the literature. Included in the study were distilled water (100 ^{o}C, 90 min), 0.2 M boracic acid in 0.05 mol/l sodium borate buffer (98 ^{o}C, 90 min), succinic acid (100 ^{o}C, 90 min), 8 M urea (80 ^{o}C, 15 min) and sodium carbonate (80 ^{o}C, 15 min). Following degumming individual fibers were subjected to tensile testing and stress-strain responses were compared. The results

as shown in Figure 4, indicated that the chemical composition, temperature and degumming time significantly impacted the strength of silk fibers. In particular the boracic buffer solution at a pH of 9.0 resulted in the highest elastic modulus, ultimate tensile strength and extensibility [59].

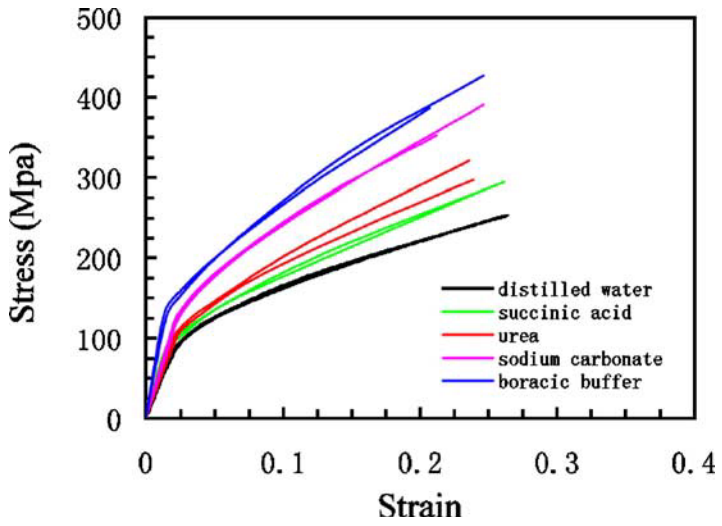

Figure 4 - Stress-strain response of silk fibers subjected to different degumming conditions. From Jiang, et al. 2006 [59].

In order to assess the inherent variability of silk tensile properties within and between cocoons, Zhao et al. unwound cocoons and performed numerous tensile tests on 5 cm segments throughout the length of the resultant fiber. As seen in Figure 5, there is significant variability in modulus, tensile strength and extensibility both within the individual fiber that makes up a cocoon and between cocoons spun by different silkworms. While the general material behavior of all fiber segments was comparable, all mechanical properties were shown to vary by nearly an order of magnitude, both within and between the silk fibers [60]

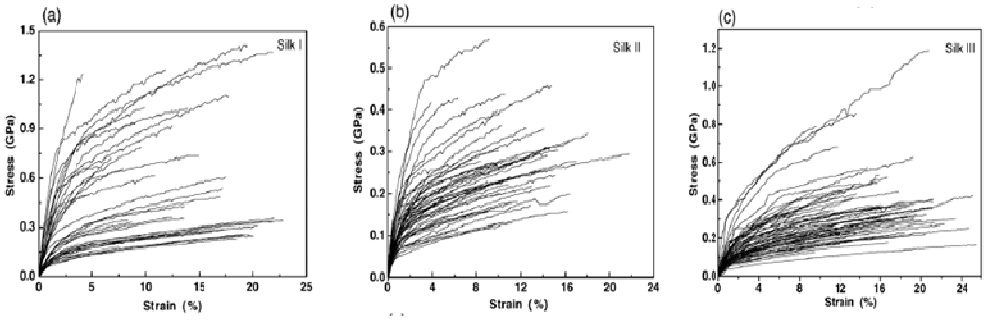

Figure 5 - Variability of silk fiber tensile behavior within a cocoon and between cocoons. (a), (b) and (c) represent different cocoons.

In addition to degumming using chemical reagents at elevated temperatures, proteolytic degumming has been proposed as a more environmentally friendly and energy efficient means to remove sericin. Freddi, et al. assessed the effectiveness of 3 different enzymes and found that the GC897-H enzyme was nearly as effective as degumming with alkali soap, with a 25% mass loss as compared with 27% for complete sericin removal with soap, as shown in Figure 6. However, the enzyme degumming can be done at significantly lower temperatures 40-60 ^{o}C versus 100 ^{o}C and with a lower volume of caustic wastes produced [61].

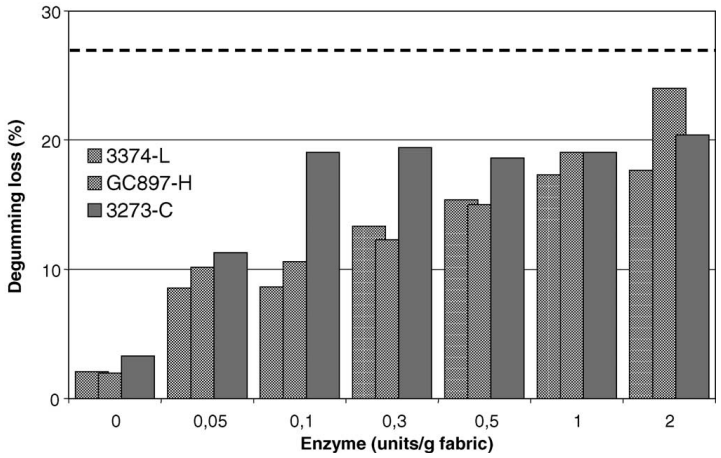

Figure 6 - Efficiency of enzymatic degumming of silk fabrics as measured by mass lost during degumming. Overbar represents the 27% mass lost during the alkali soap degumming process. From Freddi, et al. 2003 [61].

While many studies have addressed the impact of altering the degumming solutions, Ho, et al. used boiling distilled water and modulated the duration of immersion silk fibers from tussah, wild type silkworms. They tested native fibers (labeled control in Figure 7) and samples that had been degummed for 15, 30, 45 and 60 minutes and found a significant decrease in mechanical properties with longer degum times. In particular there was a substantial decrease in tensile strength and modulus when the dwell time was increased from 15 to 30 minutes [62] as seen in Figure 7.

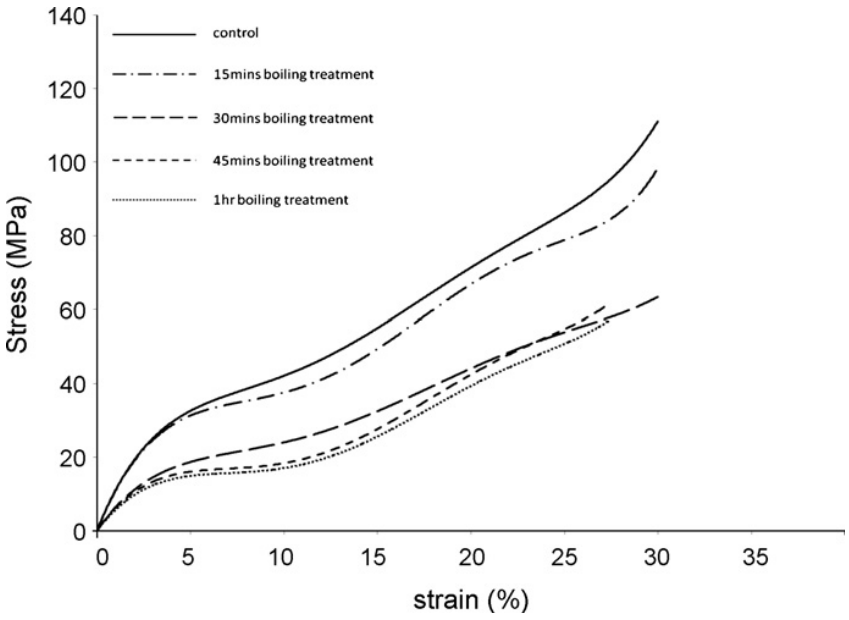

Figure 7 - Stress-strain response of Tussah silk fibers exposed to different degumming durations. From Ho, et al. 2012 [62].

2.2.2. Minimizing Protein Degradation

Researchers in the textile industry have addressed the impact degumming has on the macroscopic mechanical properties of silk fibers. However, the degumming process also affects the micro-scale properties of the silk proteins. In particular the molecular weight of the dissolved proteins is substantially degraded versus that of the silk spinning dope removed directly from the silkworm's gland. In order to characterize the degree of degradation caused during reconstitution, researchers have assessed the molecular weight of silk solutions with different process conditions.

In an effort to create functional silk fibroin solutions with molecular weights on par with those extracted from the silkworm, Yamada, et al. tested a number of different cocoon sources, degumming times, temperatures and solutions and solvents. They analyzed a number of solutions from fresh cocoons and reeled silk, degummed with urea, alkali soap, sodium carbonate, proteolytic enzymes and dissolved with a ternary solvent of $CaCl_2$/ethanol/water and lithium thiocyanate (LiSCN). This multi-factorial approach led the authors to conclude that every step in the silk reconstitution process results in degradation of the fibroin. In order to minimize this degradation the authors suggest that fresh cocoons should be degummed with 8M urea and dissolved in LiSCN. The results of these tests and the high molecular weight of the solution produced with the recommended procedure can be seen in the distinct bands near 400 kDa in the electrophoretic gel in Figure 8 [58].

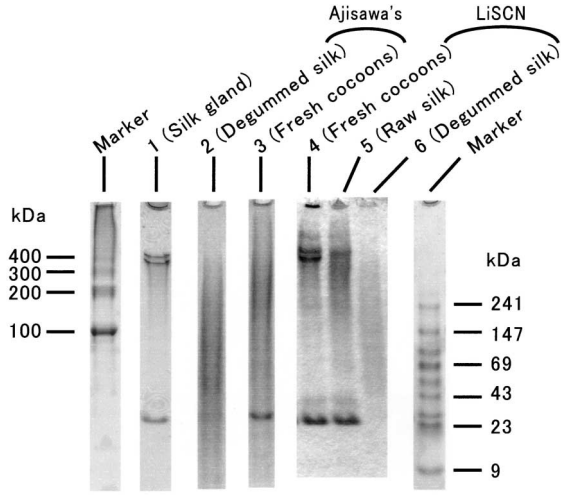

Figure 8 - Gel elecrophoresis visualization of silk proteins solutions reconstituted from different cocoon sources using various degumming and dissolution processes. From Yamada, et al. 2001[58].

Wray, et al. also addressed the degradation of silk proteins during degumming, assessing molecular weights of solutions degummed from 5 to 60 minutes in 0.02 M Na_2CO_3 solutions at boiling conditions. The results showed a shift toward lower molecular weights as the boiling time was increased. However, there was not a concomitant change in the conformation of the proteins as measured with FTIR. Figure 9 shows the results of gel electrophoresis and gel permeation chromatography analyses [63].

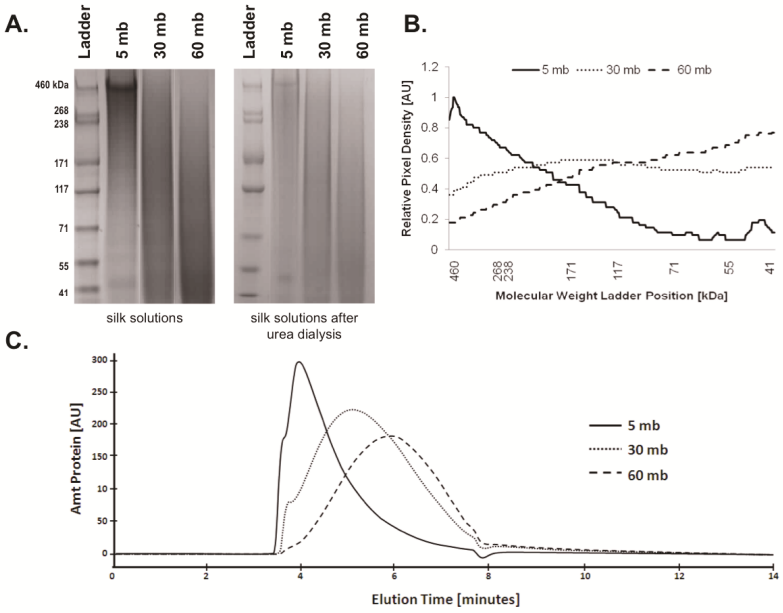

Figure 9 - Visualization of silk fibroin degradation with increased degumming times. (A) Gel electrophoresis of 5mb, 30mb and 60mb solutions. (B) Pixel density analysis of image from A. (C) Elution times from gel permeation chromatography. From Wray, et al. 2011 [63].

2.2.3. Enhancing Extensibility

One of the properties of silk that makes it useful for numerous applications is its overall toughness, or its ability to absorb energy without failure. This property is directly related to the fibroins extensibility. However, reconstituted silks are typically brittle under ambient, dry conditions. In order to improve the functionality of regenerated silks in their dry state, the extensibility of the materials needs to be increased toward that of the native silk fiber. Recent efforts have shown that the best method for improving silk film or fiber extensibility is to draw the specimen in the presence of a plasticizer after it has been formed.

Controlled drawing of rehydrated silk films after casting and ethanol treatment was shown to improve tensile strength, elastic modulus, extensibility and tenacity by Yin, et al. Specifically silk films of 200 µm thickness were cast

from solutions that had been degummed twice for 30 minutes each, were rendered insoluble with ethanol treatment and allowed to fully rehydrate for 30 minutes in distilled water. The films were then stretched to 2 or 3 times their original lengths, allowed to dry and subjected to tensile testing. Results of these tests for both the orientation of drawing and perpendicular to the draw direction are shown in Table 2 [45]. The results clearly suggest that molecular alignment is critical to produce mechanical properties similar to those of native silk fibers.

Table 2 - Mechanical properties of silk films of different draw ratios. As cast, ethanol treated (RSF-E), 2X draw (RSF-E-2) and 3X draw (RSF-E-3) both parallel (//) and perpendicular (⊥) to the prestretching direction. From Yin, et al. 2010 [45].

sample[a]	strain at break (%)	yield stress (MPa)	ultimate stress (MPa)	Young's modulus (GPa)	energy to break (kJ/kg)[b]
as-cast ($n = 12$)	5.0 ± 1.1		80 ± 10	2.7 ± 0.3	1.9 ± 0.7
RSF-E ($n = 9$)	5.1 ± 0.6		90 ± 7	2.7 ± 0.3	2.1 ± 0.3
RSF-E-2 // ($n = 11$)	20.6 ± 5.7	131 ± 18	132 ± 19	3.0 ± 0.4[c]	17.6 ± 6.6
⊥ ($n = 7$)	4.3 ± 0.7		67 ± 12	2.5 ± 0.4	1.0 ± 0.3
RSF-E-3 // ($n = 8$)	34.9 ± 6.8	167 ± 17	169 ± 11	3.5 ± 0.5[d]	38.9 ± 8.7
⊥ ($n = 6$)	3.2 ± 0.2		66 ± 11	2.6 ± 0.3	0.8 ± 0.2

Extensibility was increased after drawing, but not the modulus or tensile strengths, in films of low β-sheet content as reported by Lu, et al. Instead of inducing β-sheet via post-treatment with ethanol to generate insoluble films, the drying kinetics were retarded during casting, which results in films with higher α content that are also insoluble in water. These films were then hydrated for 30 minutes and stretched to 200% of their initial length. As seen in Figure 10, extensibility was increased by a factor of 10, while modulus and strength were halved [64].

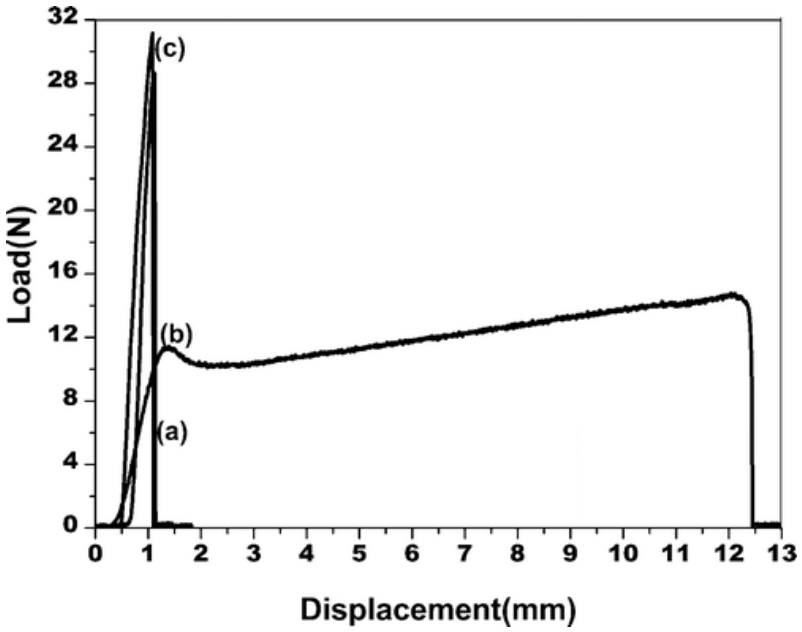

Figure 10 - Load-displacement curves for silk I films of different post treatment. (a) Methanol treated (b) 2X drawn in hydrated condition (c) As cast. From Lu, et al. 2012 [64]

2.2.4. Optimizing Regenerated Fibers

One widely researched application of regenerated silks is the ability to consistently produce regenerated fibers that meet or exceed the properties of native silk fibers. One group has claimed to have been able to produce fibers with greater strength and toughness [65]. However, they have not published subsequent work confirming and expanding on the methods and results of their original study.

In order to produce these fibers the authors extruded concentrated, regenerated silk solutions through a custom spinneret into a bath of heated ammonium sulfate at 60 ^{o}C. The fibers were then subjected to multiple drawing steps resulting in fibers with draw ratios of 1x, 2x, 4x and 6x the original extruded length. As can be seen in Table 3, the authors suggest that properties can be

controlled and optimized by altering the draw ratios. Depending on the degree of elongation one can optimize for breaking stress or extensibility [65].

Table 3 - Mechanical properties of regenerated silk fibers extruded into a 60 °C ammonium sulfate bath and subjected to different draw ratios. Adapted from Zhou, et al. 2009 [65].

Sample	Average Diameter (μm)	Breaking Stress (Gpa)	Breaking Strain (%)
RSF-1x	30.9 ± 2.0	too weak to measure	
RSF-2x	22.6 ± 2.1	0.09 ± 0.02	3.1 ± 0.9
RSF-4x	13.2 ± 2.8	0.26 ± 0.01	78.9 ± 4.8
RSF-6x	10.8 ± 2.4	0.45 ± 0.02	27.7 ± 4.2
B. mori cocoon silk	20.5 (major axis) 15.3 (minor axis)	0.40 ± 0.02	19.7 ± 1.3

Other groups attempting to produce regenerated fibers have failed to match these properties and generally report tensile strengths on the order of 60 – 150 MPa [66-69], which are more in line with what is reported for silk film behavior. This suggests that there are fundamental material differences between regenerated and native silk fibroins. Thus, given the inability of others to replicate the phenomenal results of Zhou, et al., our ability to consistently produce native-like silk fibers is still an open question.

2.3. Rationale for Experimental Design

As outlined above, a number of researchers have attempted to optimize the mechanical properties of regenerated silk fibers and films in order to match the extensibility and tensile strength of the native fiber. Some have used harsh chemical solvents [67, 68, 70], others have used drawing to align the molecules [45, 64] and others have combined both drawing and chemical treatment [65]. Despite this concerted effort to recapitulate the native silk fiber properties only

Zhou, et al. [65] have claimed to have produced fibers that approach the toughness of fibers spun by the *Bombyx mori*. Additionally, researchers in the field of textile engineering have thoroughly investigated the impact of degumming on the tenacity of silk fibers [59, 71]. Further, research has been undertaken to understand the degradation of the silk fibroin during the reconstitution process [58, 63].

Despite these different efforts, to date no research has been found that addresses the impact of silk processing and particularly molecular weight preservation, in addition to post-process drawing has on the regenerated silk construct. The cast film was chosen as the optimal format for testing processing impacts as it is easily produced, imparts minimal confounding variables and results in relatively consistent samples. These films were steam drawn in order to induce alignment of the molecules. Steam was chosen as the preferred plasticizer for drawing as it does not necessitate the film to be water insoluble. Insoluble films require treatment with methanol or water annealing which locks in the structure of material. By avoiding this step we increase the mobility of the molecules and should allow for a greater degree of workability and increased molecular alignment.

3. Solution Properties

3.1. Materials and Methods

3.1.1. Silk Processing

All silk solutions used were processed in general accordance with the procedures described by Rockwood, et al. [55], as depicted in Figure 11. Briefly, 5 grams of *Bombyx mori* cocoons (Tajima Shoji, Japan) were cut into quarters and the silkworm and residue were removed. The cut and cleaned cocoons were weighed, the mass recorded and the cocoons immersed in 2 liters of Milli-Q water (EMD Millipore, Billerica, MA) with 4.24 g Na_2CO_3 (Sigma Aldrich, St. Louis, MO). The 0.02 M Na_2CO_3 degumming solution with cocoons were boiled for 2.5, 5, 10, 15, 20, 30, 60 or 90 minutes or held at 70 ^oC for 60, 90, 120, 150, 180, 210, 240 or 270 minutes. These groups will hereafter be referred to as 2.5mb, 5mb, etc. where the "mb" stands for "minutes boiled" or 70C-60m, 70C-90m which signifies the duration in minutes the silk was immersed in 70 ^oC Na_2CO_3 solution. Following degumming, the silk fibers were rinsed three times, for 30 minutes each, in 1 liter of Milli-Q water. The thoroughly rinsed fibers were removed, wrung out, and placed in a hood to dry for at least 36 hours. After drying the fibers were weighed and the final degummed weight and mass lost recorded.

The degummed silk fibers were then dissolved in 9.3 M LiBr (Sigma Aldrich, St. Louis, MO) at 60 ^oC for 4 hours at a 15 % weight/volume ratio. Following solubilization, 12 ml of the fibroin solution was injected into a regenerated cellulose dialysis cassette (3,500 MWCO, Slide-A-Lyzer, Pierce, Rockford, IL) and dialyzed against Milli-Q water for 48 hours. The dialysate was

changed after 1, 6, 12, 18, 24, 30, 36 and 42 hours. In order to minimize shearing, the silk solution was removed from the cassette by carefully puncturing the dialysis membrane and collecting the solution in a beaker. The solution was then centrifuged twice at 14,000 rpm, for 20 min. at 4 ^{o}C using a Sorvall RC-5B refrigerated superspeed centrifuge and SS-34 rotor. Following centrifugation, solution concentration was determined by drying 0.5 ml aliquots and the solutions were stored at 4 ^{o}C and were used within one week of generation.

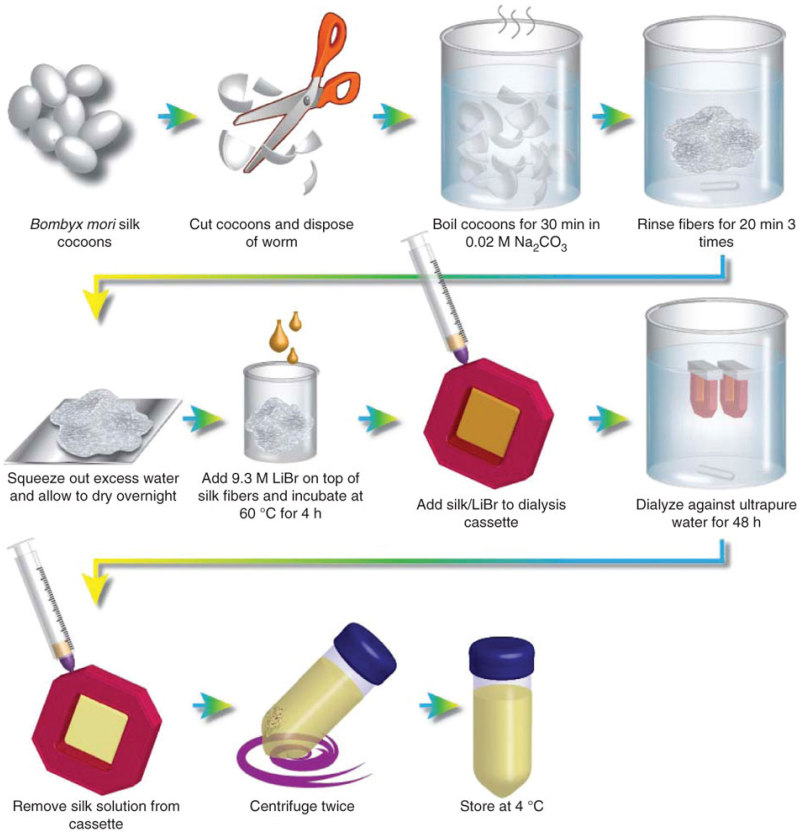

Figure 11 - Schematic of the silk fibroin reconstitution procedure. From Rockwood, et al. 2011.

3.1.2. Sericin Content

Sericin content of the solutions was determined by calculating the percentage mass lost during the degumming process and comparing it to the average 26.3% sericin for Japanese cocoons. Silk cocoons were massed prior to degumming and following complete drying after removal of the sericin coating. All data represent n=6 for boiled conditions and n=3 for 70 ^{o}C conditions. Percent residual sericin was calculated using the following formula

$$\%\ sericin\ = \frac{26.3\% - \%\ mass\ loss}{26.3\ \%}$$

3.1.3. Gel electrophoresis

The electrophoretic mobility of the fibroin molecules was determined using sodium dodecyl sulfate polyacrylamide gel electrophoresis (SDS-PAGE). For each condition of interest 5 µg of silk protein was reduced and loaded into a 3-8% Tris Acetate gel (NuPAGE, Life Technologies, Grand Island, NY). The gel was run under reducing conditions for 45 minutes at 200 V, with a high molecular weight ladder as a reference (HiMark Unstained, Life Technologies) and stained with a Colloidal Blue staining kit (Life Technologies). The molecular weight distributions of the silk solutions were determined by imaging the gels, performing pixel density analyses and normalizing across all the lanes for a peak intensity value of one (ImageJ, NIH, Bethesda, MD).

3.1.4. Viscosity

Silk solutions were diluted to a concentration of 5% w/v, gently mixed and allowed to equilibrate over night at 4 ^{o}C. The following day the solutions were slowly brought to room temperature (25 ^{o}C) and dynamic viscosity of the solutions was tested using an RVDV-II+ cone and plate viscometer (Brookfield Engineering, Middleboro, MA). For solutions with a plastic viscosity above 20 cP, testing was done using a CP-52 cone, with a 1.2 cm cone radius and 3^{o} cone angle over a shear rate range from 10 – 300 1/s. Solutions with a plastic viscosity below 20 cP were tested using CP-40 cone, with a 2.4 cm radius and 0.8^{o} cone angle over a shear rate range of 37.5 – 1500 1/s. Following collection of the shear rate and torque, the data was analyzed and fitted using the Bingham Plastic model using Rheocalc V3.3 software (Brookfield Engineering). The Bingham plastic model assumes a Newtonian fluid behavior after an initial yield stress is overcome. The data is fitted to the equation

$$\tau = \tau^{o} + \eta D$$

where τ is the measured shear stress, τ^{o} is the yield stress, η is the plastic viscosity and D is the shear rate.

A representative screenshot of the Rheocalc software analysis tab showing the interface and values reported is provided in Figure 12. During the analysis procedure the first two data points of each sample were removed to allow for full engagement of the sample with the cone. In addition samples that exhibited signs of gelation, a rapid increase in shear stress, were eliminated and the tests repeated. Data represents three samples from three separate batches of silk solution.

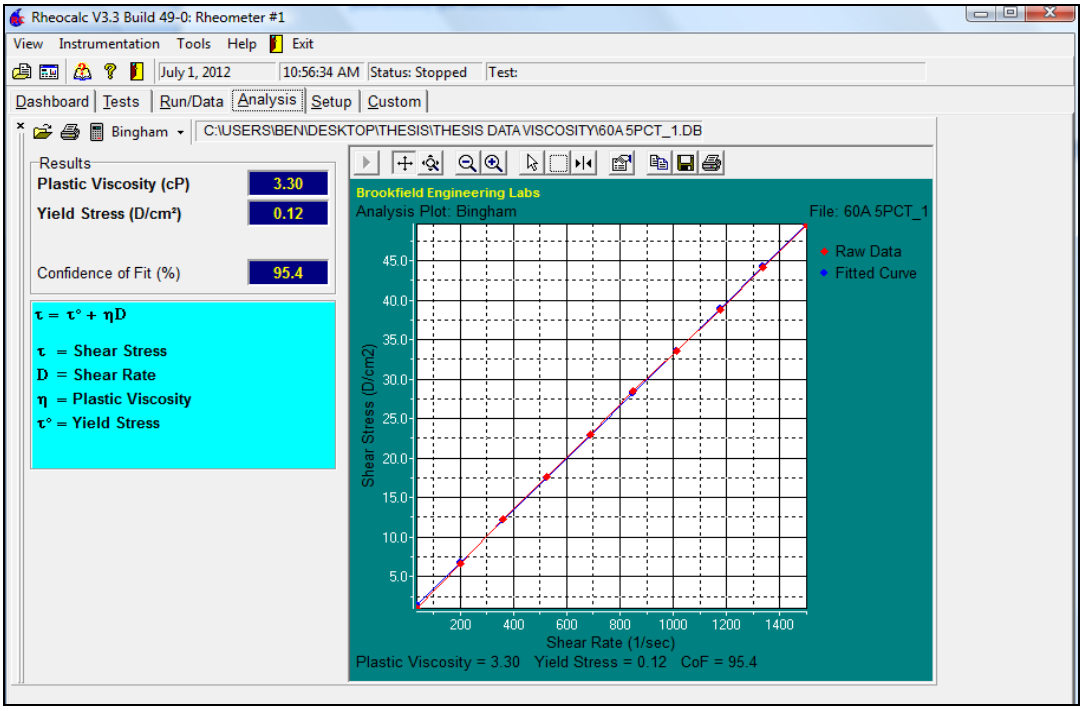

Figure 12 - Screenshot of Rheocalc software used for analysis of all viscosity data. Analysis assumed a Bingham plastic behavior, with Newtonian behavior following an initial yield stress.

3.1.5. Rheometry

Rheological measurements were taken using an ARES strain-controlled rheometer (TA Instruments, New Castle, DE). Dynamic oscillatory frequency sweeps were taken using a 50 mm parallel plate geometry at room temperature (25 ^{o}C). The silk solution was loaded onto the bottom platen in a manner as to minimize shear and the upper platen was lowered to a gap distance of 0.5 mm with a maximum applied normal force of 0.05 N. The viscoelastic response of the silk solution was recorded with a strain magnitude of 1% and a wide range of frequencies from 0.1 - 100 rad/s. All solutions were at a concentration of 7.5% and were tested within 3 days of being removed from dialysis, the final stage of silk solution processing.

3.2. Results

3.2.1. Sericin Content

Effective removal of the sericin protein from the silk fibers is a fundamental step in preparing solution for use *in vivo*. The results of mass loss experiments indicated that sericin is substantially removed from the fibers after degumming for 2.5 minutes at a boiling temperature and after 60 minutes when held at 70 ^{o}C, as can be seen in Figure 13.

For the boiling condition there were no statistically significant differences ($p > 0.05$) between the 2.5mb, 5mb, 10mb, 15mb, 20mb and 30mb groups. However, the 60mb and 90mb groups were significantly different ($p < 0.01$) than all shorter degumming times, losing approximately 1% more mass than the other 6 conditions. This additional mass loss is likely due to the substantial degradation of the fibroin as the degumming time is increased, allowing small fragments to be removed during the rinsing steps.

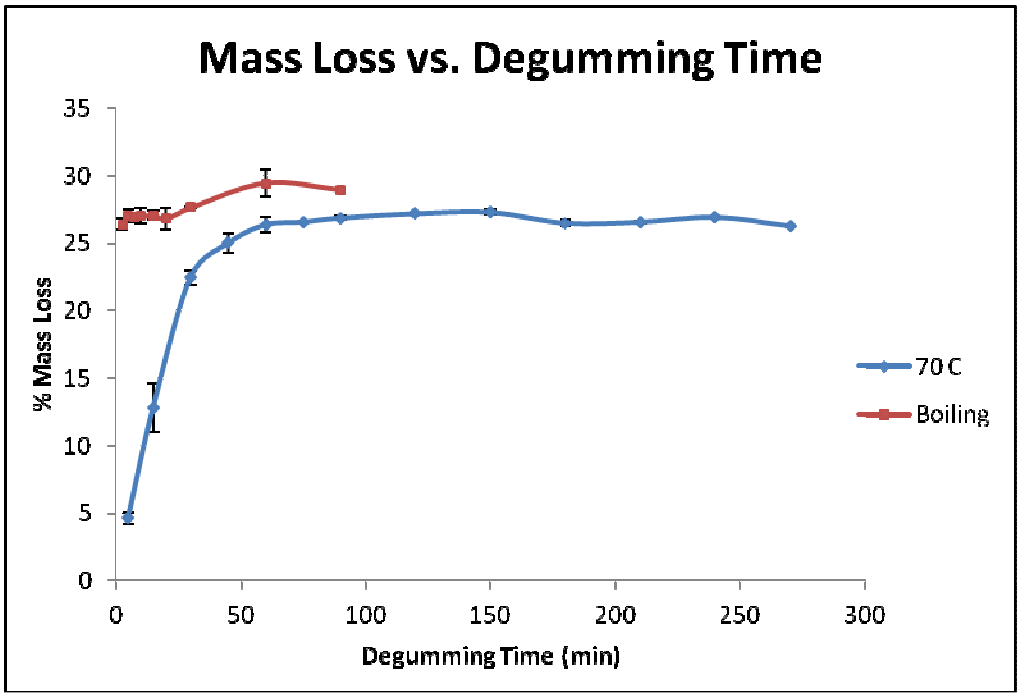

Figure 13 - Mass lost during degumming of Japanese cocoons in boiling or 70 ^{o}C 0.02M Na_2CO_3 solution for various durations. Mass loss can then be used to calculate residual sericin content, using an original value of 26.3% of the starting mass is sericin.

The 70 ^{o}C degumming in 0.02 M Na_2CO_3 solution resulted in substantial sericin removal in approximately 60 minutes, with statistically significant additional mass loss ($p < 0.05$) occurring at durations of 120 and 150 minutes. For both these groups an additional 0.5% of the initial fiber mass was lost during the degumming process. The 270 minute group exhibited a significant decrease in mass loss ($p < 0.05$) as compared to the 90, 120, 150 and 240 minute groups. In addition to the verification of at least 26.3 % loss of initial mass, the percent residual sericin was calculated for the 70 ^{o}C – 5, 15, 30 and 45 minute groups as shown in Table 4. These calculations indicate that the amount of sericin removed is roughly proportional to the amount of time it is exposed to the 70 ^{o}C, sodium carbonate degumming solution.

Table 4 - Residual sericin content for short duration degumming in 70 ^{o}C sodium carbonate solution.

Degum Time at 70 ^{o}C	% Mass Loss	% Residual Sericin
5	4.6%	82.5%
15	12.8%	51.5%
30	22.4%	14.7%
45	25.0%	5.1%
60	26.3%	0.0%

3.2.2. Molecular Weight

Increased degumming times and temperatures of the silk fibers correlated directly with a decrease in the average molecular weight of the protein which is shown by the downward shift of the smear exhibited on the SDS-PAGE gels. This degradation with longer degum times is clearly shown for both boiling temperatures and 70 ^{o}C degum conditions in Figures 14 and 15 respectively.

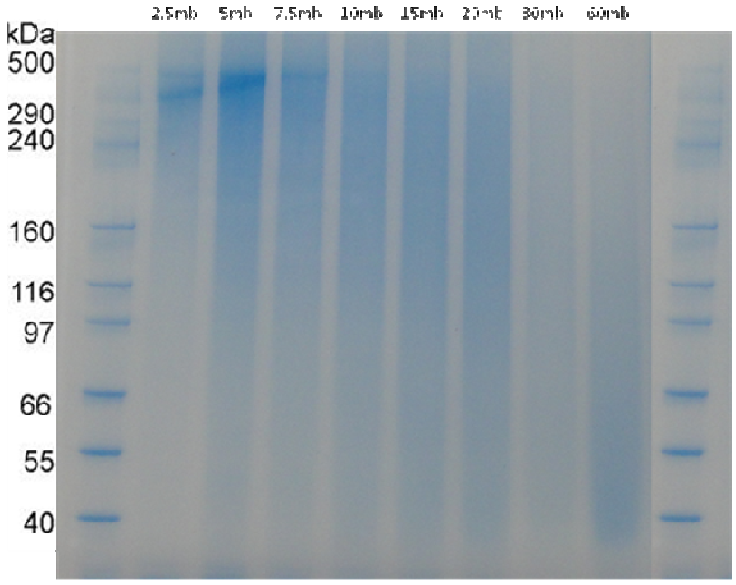

Figure 14 - Image of SDS-PAGE gel for solutions that were degummed in sodium carbonate at boiling temperatures.

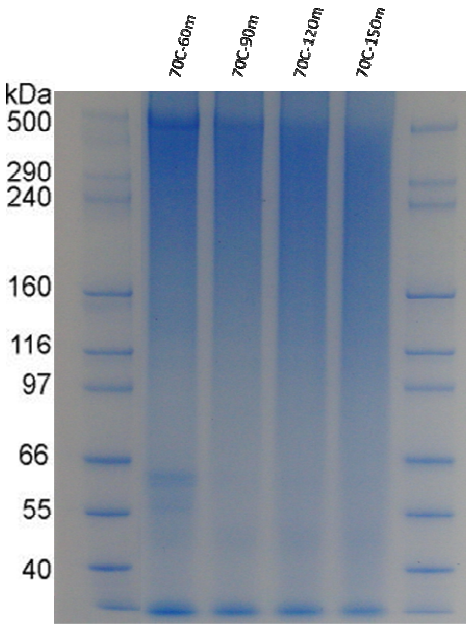

Figure 15 - Image of SDS-PAGE gel for solutions degummed in sodium carbonate at 70 ^{o}C.

In addition to qualitative visual analysis, densiometric image analysis was performed on the electrophoresis gels. The raw pixel intensity for each lane was collected and the intensity values were normalized across all data groups to provide an intensity range from 0 to 1. Following normalization of the data, pixel intensity for each group was plotted against the vertical lane position as shown in Figure 16. This clearly shows that the bulk of the proteins in low degumming conditions including 2.5mb, 5mb, 70C-60m and 70C-90m (not all data shown) are in the high molecular weight bands at approximately 500 kDa. At 10 min of degumming the pronounced peak at approx. 500 kDa has been eroded and the molecular weight distribution becomes more distributed between approx 500 to 100 kDa. At 30 minutes of boiling the protein is degraded to where its distribution is nearly equal across the whole range of weights visualized by the gel, including down to the 40 kDa range. Degumming for 60 minutes resulted in

a pronounced shift in the molecular weight distribution of the silk solution, with a peak concentration occurring at approximately 60 kDa. The relative degradation profile of the silk solutions degummed at 70 ^{o}C is similar to that for boiled solutions, however, the kinetics are significantly retarded. This is clearly indicated by the paralleling of the 70C-60m group with the 2.5mb group in Figure 16.

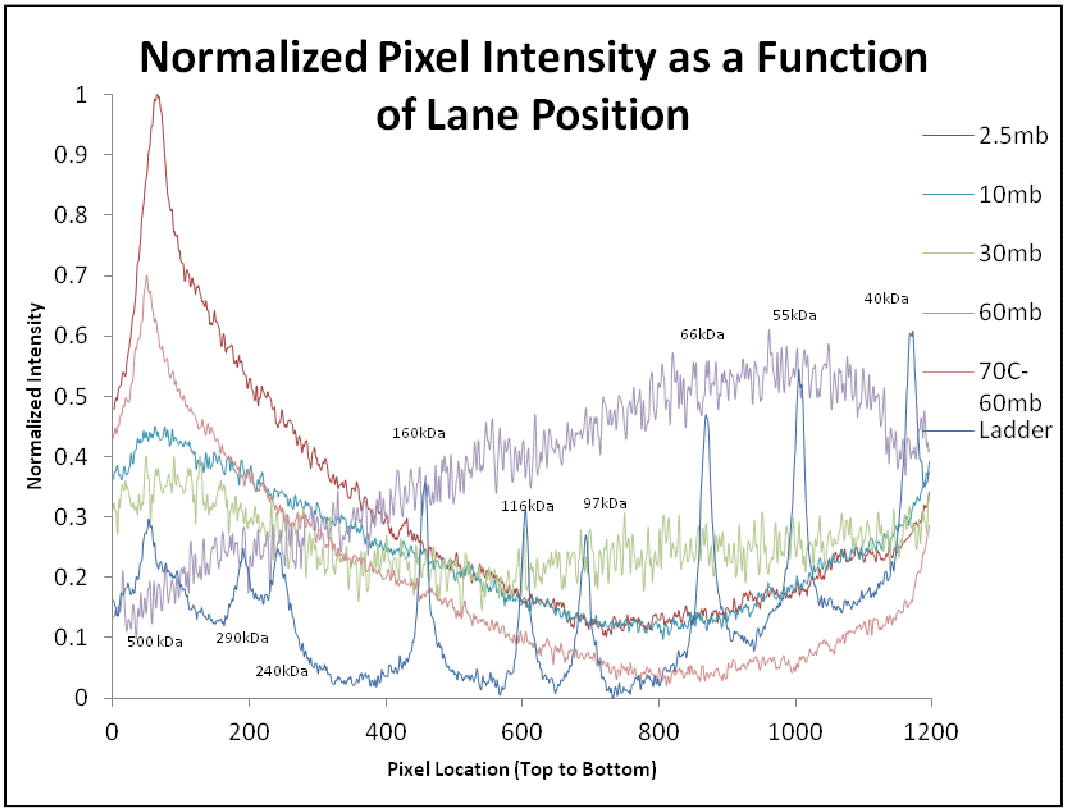

Figure 16 - Image analysis of SDS-PAGE gel showing normalized pixel intensity with respect to lane position. Ladder peaks indicating molecular weight are shown.

Figure 17 presents the densiometric analysis while also accounting for differences in protein loading between the lanes. This was accomplished using a binning process to sum intensity contributions into molecular weight bins delineated by the peaks in the ladder. For each experimental group, the

contribution of protein from each molecular weight bin was then divided by the total of all bins to provide the relative amount of protein in that molecular weight band. This analysis further clarifies the substantial impact on the molecular weight from additional degumming times. In addition it suggests that the 70 ^{o}C degumming temperature may result in less degradation to the protein molecule as there is less of a contribution to the overall loading from bands below 160 kDa.

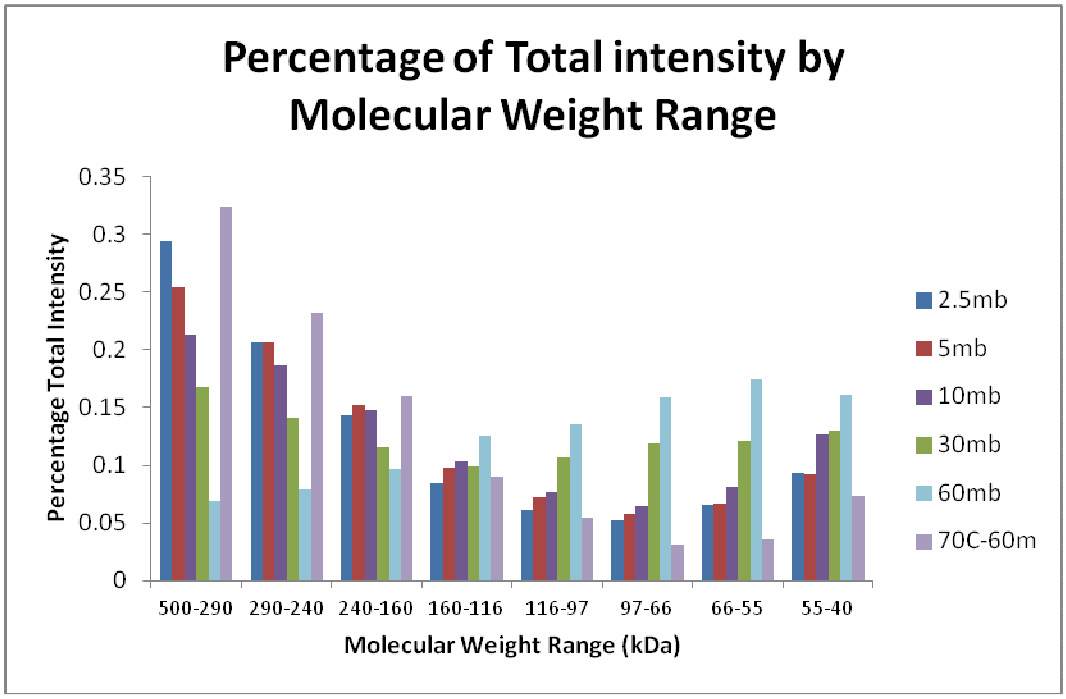

Figure 17 - Molecular weight distribution of differently degummed solutions as a percentage of total pixel intensity per SDS-PAGE lane.

3.2.3. Rheological Behavior

The plastic viscosity of solutions, produced from a wide range of degumming conditions, was characterized as shown in Figure 18. The viscosities exhibited a roughly exponential behavior with a rapid decrease from a maximal

plastic viscosity of 113 cP for 2.5mb solution to a low of 3.3 cP for 60mb solution. The same behavior was seen with the 70 ^{o}C solutions with a plastic viscosity of 48 cP for 70C-120m solution to 8.77 cP for 70C-270m solution. Note that viscosities were not collected for the 70C-60m and 70C-90m groups as there was a propensity for the solutions to gel upon the application of any shear which prevented consistent data collection.

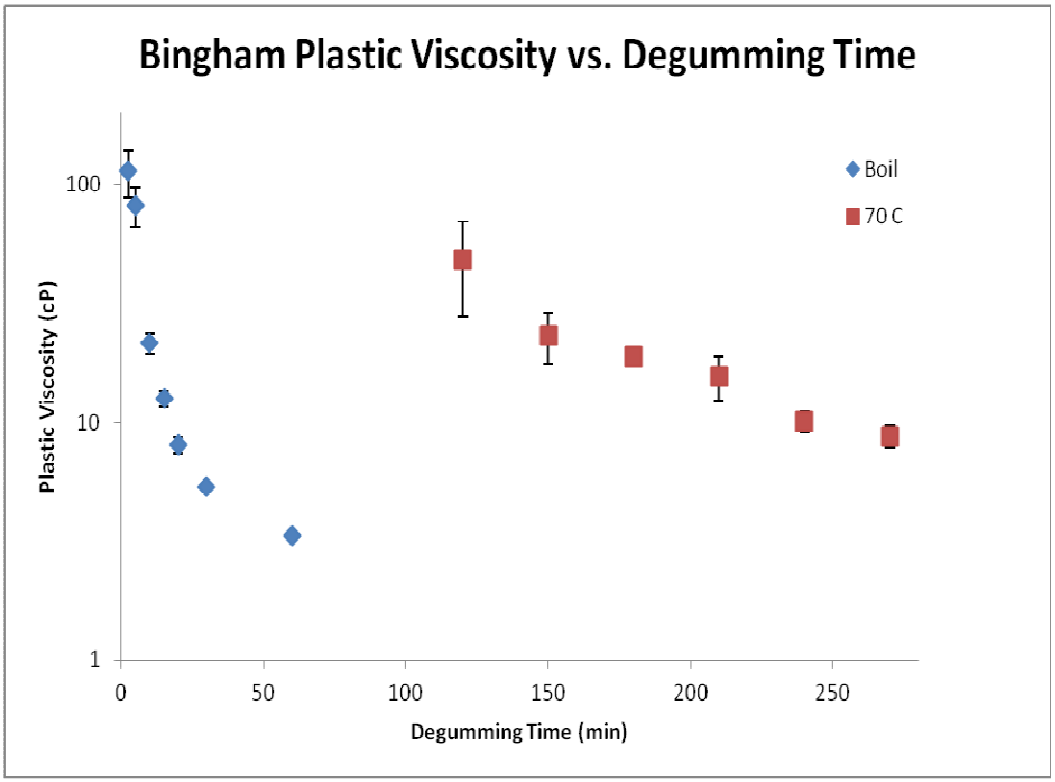

Figure 18 - Bingham plastic viscosity as a function of different degumming times and temperatures.

Full rheological behaviors of solutions were collected over a wide range of degumming conditions. The rheological data allows for greater insight into the solution behavior, quantifying the degree of elastic behavior as the storage modulus (G') and viscous behavior as the loss modulus (G"). As shown in Figure

19, the storage and loss moduli for 5mb, 10mb, 30mb and 60mb cover a range of three orders of magnitude from 0.1 to 100 Pa and indicate a storage modulus greater than the loss magnitude. This indicates that the solutions are acting more like a “solid” or “elastic” material than that of a viscous liquid. The only sample that does not exhibit this behavior is the 60mb group; however, the torque values are below the minimum range of the instrument and are of suspect validity. In addition it is interesting to note that the 5mb and 10mb groups show similar behaviors and magnitudes despite the fact that the 10mb sample was exposed to twice the degumming time which should cause greater degradation and lower magnitudes of G’ and G”.

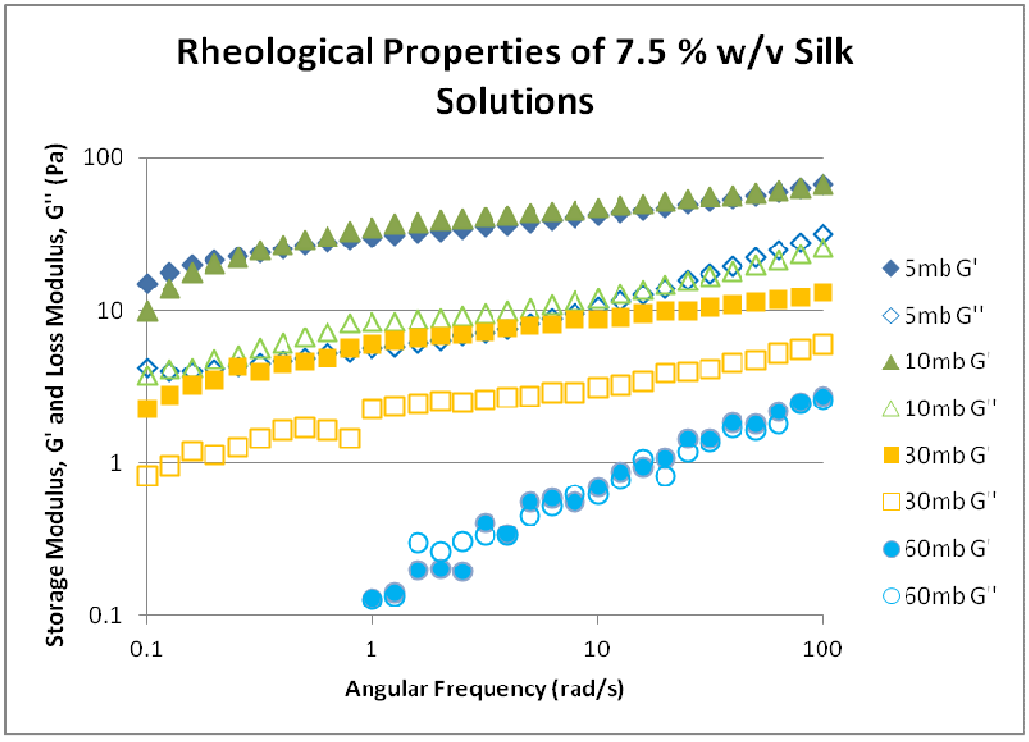

Figure 19 - Rheological properties of differently degummed silk solutions. Storage modulus (G') and Loss modulus (G") are shown in solid and open markers respectively.

3.3. Discussion

The established method for measuring degumming efficiency has been accepted as the measurement of the mass of the fibers that has been lost during processing [46]. This presumes that the relatively hydrophilic sericin components are preferentially stripped from the water stable fibroin proteins. However, as degumming time at boiling conditions is increased to 60 minutes and beyond there is actually an apparent decrease in degumming effectiveness. This can be seen in Figure 13 and is also reported by Yamada, et al., where they show a decrease in degumming efficiency from 25.8% to 22.6% with an increase from 20 to 60 minutes of immersion in Na_2CO_3. This increase in mass is unlikely to be associated with an actual increase in protein volume and instead suggests the breaking of bonds within the fibroin structure which would allow for the presence of more bound water.

Molecular weight analysis and viscosity data confirm that as degumming time and temperature are increased the fibroin proteins are subject to greater degradation. While the rates of degradation are significantly slower at 70 ^{o}C versus boiling, the general trends are consistent with the sharp band near the 500 kDa marker at low degum times slowly spreading and shifting downward as immersion times increased.

One potential concern with the SDS-PAGE gels is that the gently degummed silks have an apparent molecular weight that is on the order of 150 kDa higher than the generally accepted 350-370 kDa for native fibroin [15, 72]. In order to allay these concerns, silk dope extracted from the *B. mori* silkworm

was tested using the same protocol and the distinct fibroin and sericin bands were shifted up by the same 150 kDa (data not shown). This discrepancy is likely due to differences in protein folding between the marker protein and silk fibroin as electrophoretic mobility is influenced by both protein folding and molecular weight [73].

Holland, et al. have previously suggested that regenerated silk solutions have fundamentally different behaviors from native dope. They offer rheological evidence to support this conclusion, whereby native silks behave like molten polymers, with distinct G'/G" crossovers and moduli of 100 – 1000 Pa at high concentrations, while regenerated solutions lack a G'/G" crossover and have moduli four orders of magnitude lower. The results shown Figure 20 suggest that using gentler degumming conditions, in the form of lower temperatures and shorter durations, results in moduli that are much closer to those of natives. The rheological data from a 5mb, 7.5% w/v solution, superimposed on Holland et al.'s data, suggest that the low degumming condition provides native-like solution properties. The 5mb solution, while of slightly higher concentration, 7.5% w/v, than Holland's native 4.6% solution, displays the same behavior and relative magnitudes.

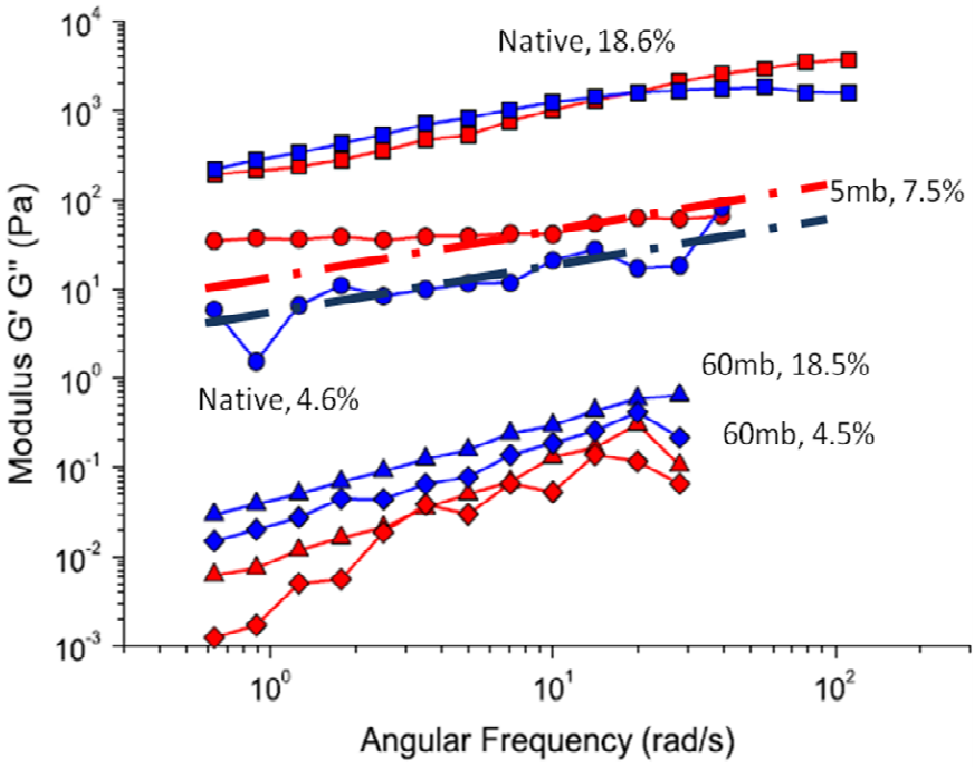

Figure 20 - Rheological data for native and reconstituted silk solutions. Storage modulus, G', depicted in red and loss modulus, G", depicted in blue. Data shown with markers are from Holland, et al. while the dashed lines represent the 5mb 7.5% w/v solution. Adapted from Holland, et al. 2007 [44]

In addition to their analogous moduli, the native 4.6% and regenerated 5mb, 7.5% solutions exhibit the same behavior. Namely, the G' and G" values are inverted, suggesting a gel like state, instead of the viscous fluid expected. This inversion of properties is likely related to entanglements between unfolded protein chains. Zainuddin, et al. have shown, in Figure 21, that this behavior is time dependent, where fresh solutions are gel like, transition to viscous fluids and return to gel like state. This behavior suggests that micelle formation is time dependent and that as a regenerated solution ages, it transitions from a random mixture of unfolded protein chains, to a highly ordered liquid crystalline solution resulting in related changes to the rheological properties [74].

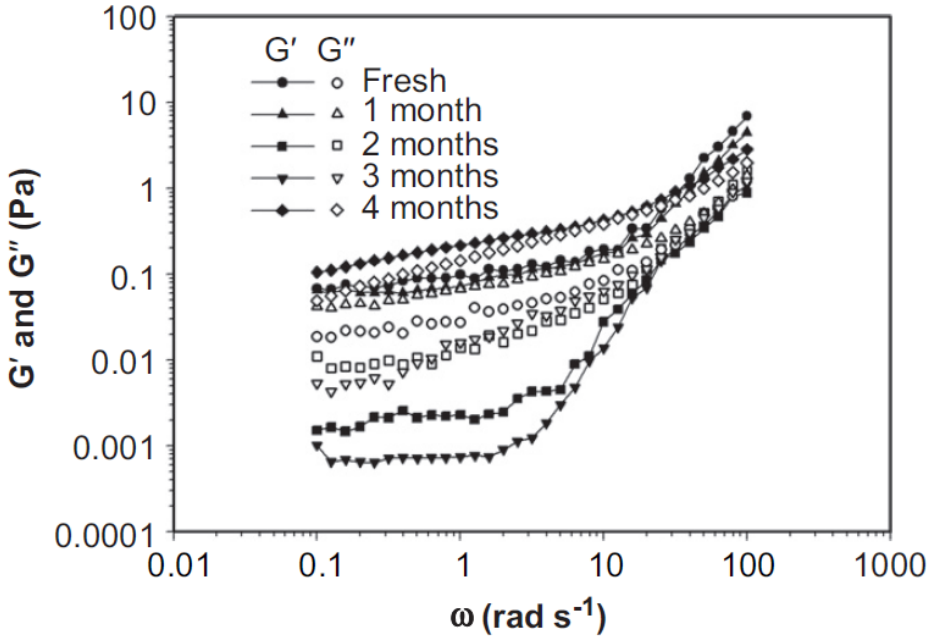

Figure 21 - Storage, G', and loss, G", moduli of fresh and aged silk fibroin solutions at 3.8% w/v. From Zainuddin, et al. 2008 [74].

4. Film Properties

4.1. Materials and Methods

4.1.1. Film Casting

Silk films were cast at room temperature (23-25 ^{o}C) and a relative humidity of 15% - 30% in 100 mm polystyrene petri dish. Based on the solution concentration, an appropriate volume of silk solution to generate a 75 µm thick film, was gently poured into the petri dish, gently spread with a pipette tip to achieve proper dispersion and any air bubbles removed. The films were allowed to dry for 24 hours before handling to ensure complete self-assembly and water evacuation and stored at room temperature and humidity. All solutions were cast within 10 days of their removal from dialysis.

Post-treatments were performed on select films to determine inter-group differences in treatment response. Films from 5mb, 15mb, 30mb and 60mb groups were treated in either methanol or water annealed to induce transition to β-sheet. Methanol treated films were cut into 6.2 mm wide strips and soaked in 100% methanol at room temperature for 4 hours. The film strips were then removed from the methanol and placed in a hood and allowed to dry overnight to allow evaporation of residual methanol. Water annealed films were cut into 6.2 mm wide strips and placed in an evacuated bell-jar container with water in the bottom, at 37 ^{o}C for 2 hours. The films were subsequently removed and allowed to dry overnight in a hood.

4.1.2. Film Drawing

After casting and appropriate drying, films were cut into 6.2 mm wide strips. These strips were hand drawn over a steam jet, as shown in Figure 22. Drawing commenced at one end of the film and proceeded along its length as the area exposed to steam reached its maximum extension. Maximum extension was determined when the application of additional tensile force or steam exposure would lead to film failure as tested in a screening strip. The distance between the grip locations was measured to the nearest millimeter before and after drawing and the draw ratio calculated as follows;

$$Draw\ Ratio = \frac{Final\ Length - Initial\ Length}{Initial\ Length}$$

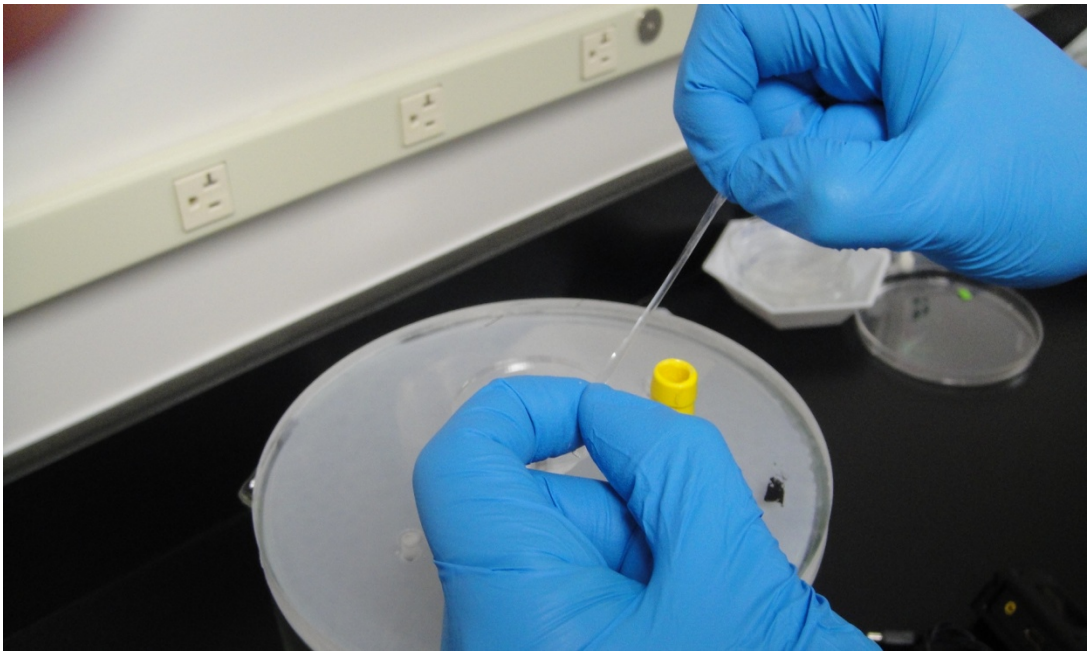

Figure 22 - Steam drawing of silk film strips. Steam jet generated by heating beaker of Milli-Q water on a hot plate with custom fitted top.

4.1.3. Tensile Testing

All tensile testing was performed as previously described [75]. Specifically, a sample of 20 mm gage length was tested at a crosshead speed of 1.2 mm/min (0.1% strain/sec) and a preload of 0.5 N, using an Instron 3366 testing frame (Instron, Norwood, MA), with 100 N load cell. To prevent slippage or failure due to stress concentration at grip edges, specimens were prepared by applying a piece of doubled over tape at each grip location. Samples were then measured for length and width, values recorded and the sample mounted in the test fixture as shown in Figure 23. The specimens were tested until failure and load and extension data collected. All testing was performed at ambient temperature and humidity.

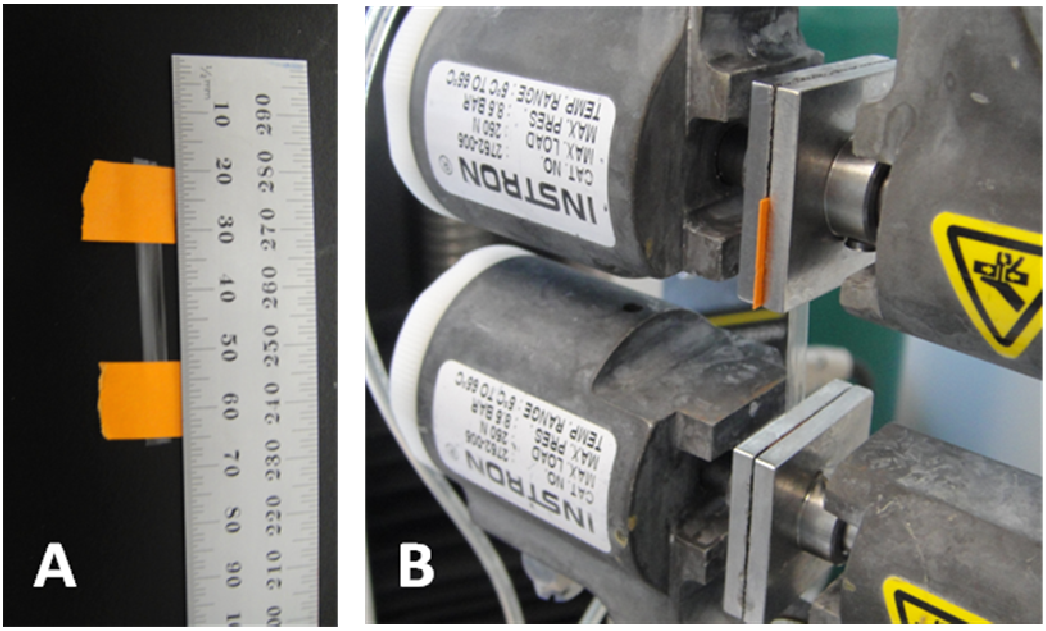

Figure 23 - Tensile test sample and fixture. (A) Sample with tape applied and ready for mounting in test fixture. (B) Sample mounted in test fixture ready for tensile test.

Tensile data was analyzed for linear elastic modulus, extensibility and ultimate tensile stress using a custom LabVIEW program. The modulus was calculated as the least squares fit between 1.5 to 3.5% strain. The extensibility was the strain achieved before a > 10% decrease in applied load and the ultimate tensile stress was taken as the maximum engineering stress achieved throughout the test.

4.1.4. Fourier Transform Infrared Spectroscopy (FTIR) Analysis

Conformational differences in the silk films were analyzed using a JASCO FTIR 6200 spectrometer (JASCO, Tokyo, Japan) with a MIRacle^{TM} attenuated total reflection (ATR) Ge crystal cell in reflection mode. Silk films were tested fully dried and at ambient conditions. Background spectra were taken and subtracted from all sample readings. Each measurement represents the average of 64 scans taken at a resolution of 4 cm^{-1} and wavenumbers ranging from 500 to 4000 cm^{-1}. Data was truncated to only include the amide I band from 1595 to 1705 cm^{-1} and peak normalized.

4.2. Results

4.2.1. Drawing Behavior

Steam drawing of the films resulted in a consistent draw ratio of 3.2 – 3.4 times the initial film length, regardless of degumming conditions, as indicated in Figure 24. The only exception to this was in the samples from the 30mb and 60mb groups which exhibited significantly greater ($p < 0.01$) draw ratios of 4 and 4.7 respectively.

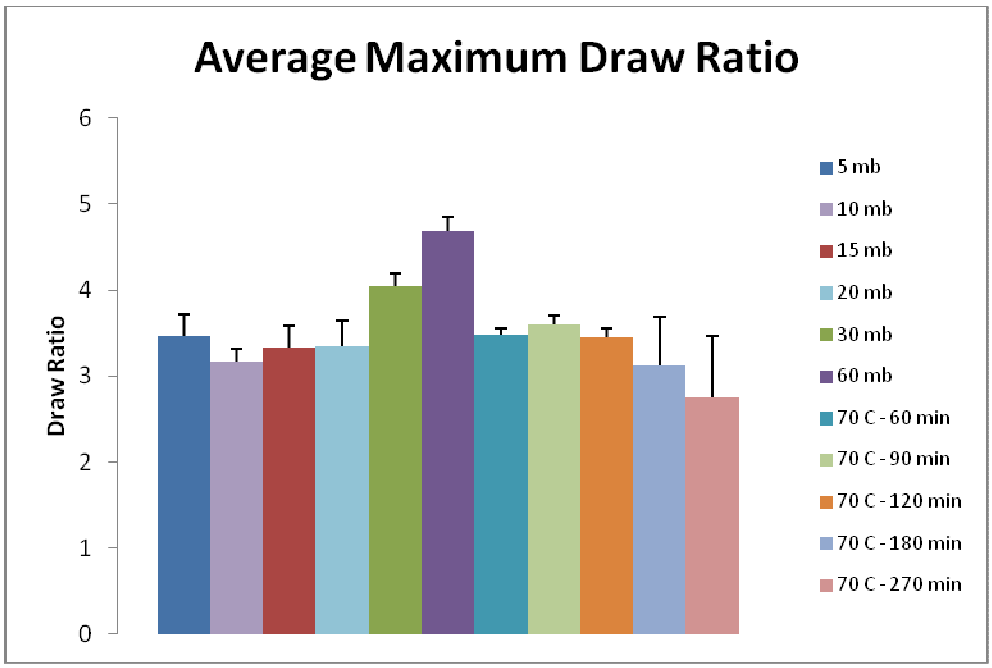

Figure 24 - Draw ratio of 6.2mm wide silk film strips as a function of degumming condition. Significant differences were found between the 30mb and 60mb groups and all other conditions, $p < 0.01$.

4.2.2. Mechanical Behavior

The linear elastic modulus, extensibility and ultimate tensile strength of differently degummed films in as cast and steam drawn conditions are shown in Figures 25, 26 and 27, respectively. Tabulated values of averages and standard deviation are also provided in Table 5. Representative stress-strain curves for as cast and steam drawn samples are shown in Figure 28.

In general, all as cast film samples, regardless of degumming conditions, exhibited a purely brittle behavior, with no distinct yield point and failure within the linear elastic region. The steam drawn samples, with the exception of the 60mb group, showed behavior more typical of a ductile material, with a prominent yield and subsequent work hardening behavior until failure. In addition to overall material behavior changes with steam drawing, the stretching

resulted in higher elastic moduli, extensibility and ultimate strengths for all experimental groups except the 70C-90m and 60mb groups. The steam drawn 70C-90m group only showed increased extensibility and tensile strength while the 60mb group only had increased modulus after drawing. The as cast modulus and steam drawn extensibility were also inversely related with the 15mb and 70C-120m groups having moduli of approximately 1 GPa with extensibilities of 40% or greater after drawing.

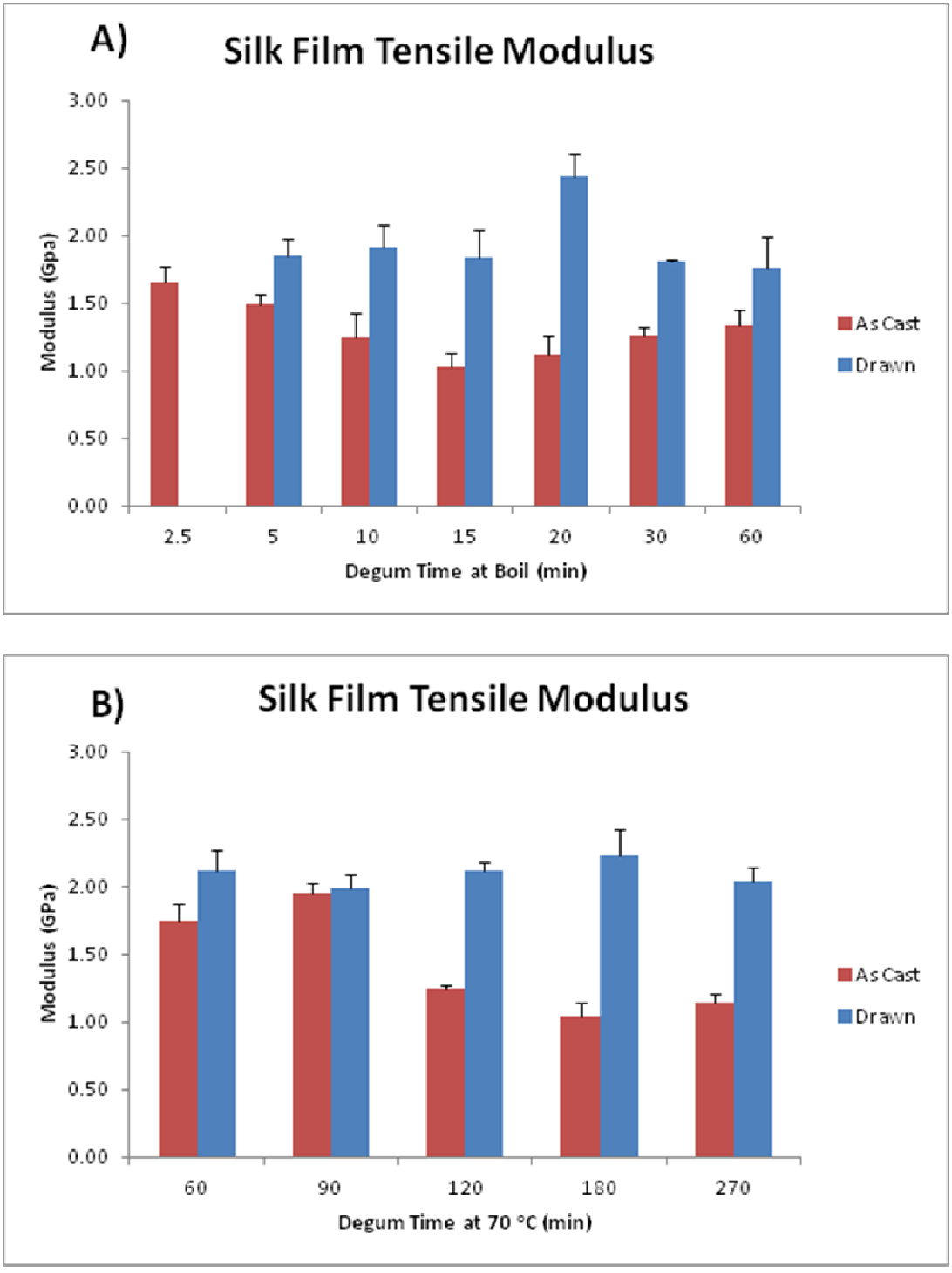

Figure 25 - Linear elastic modulus of silk films in as cast and steam drawn states. (A) Films of different degum times at boiling temperature. (B) Films of different degum times at 70 ^{o}C.

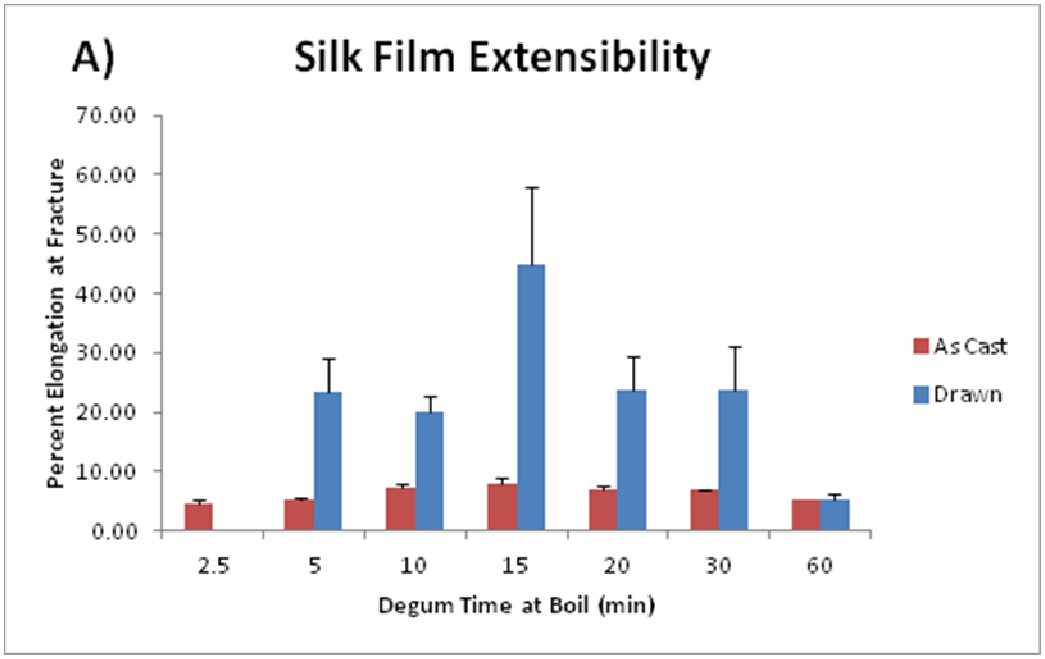

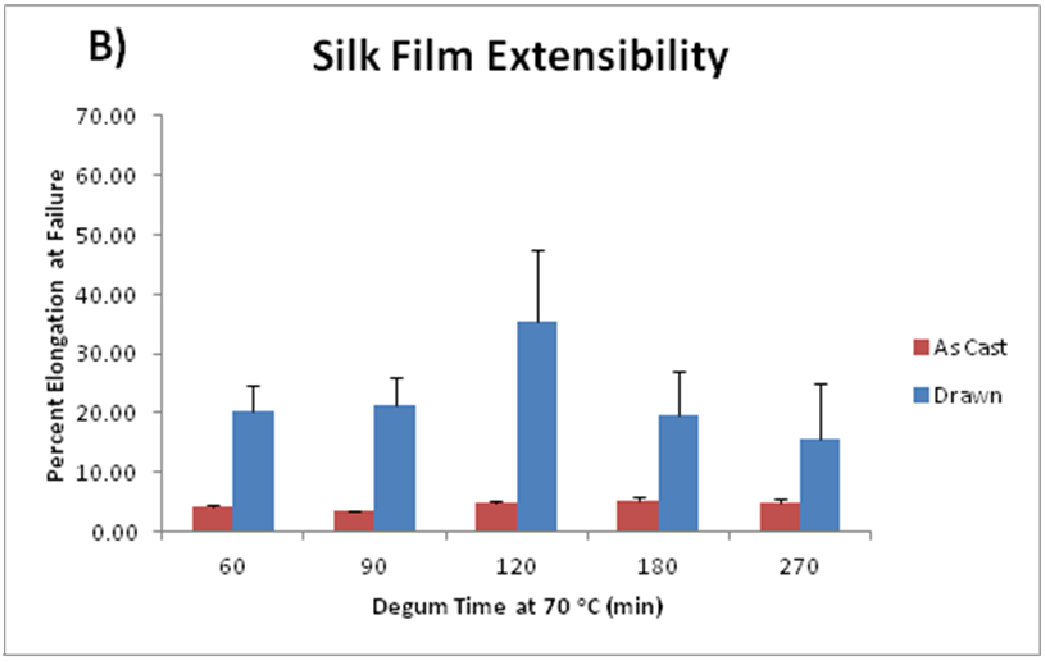

Figure 26 - Maximum extensibility of silk films in as cast and steam drawn states. (A) Films of different degum times at boiling temperature. (B) Films of different degum times at 70 °C.

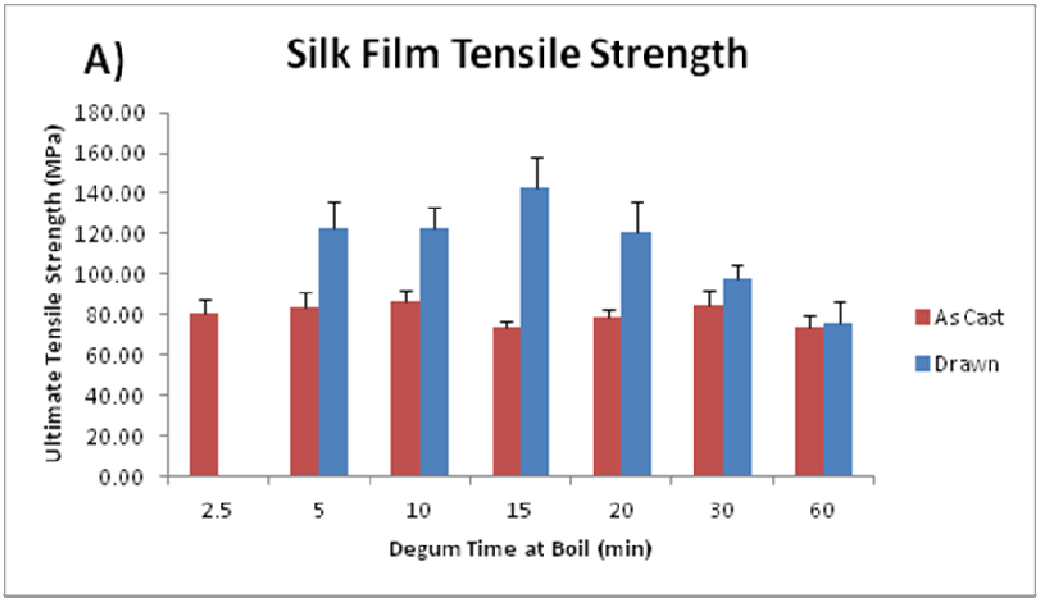

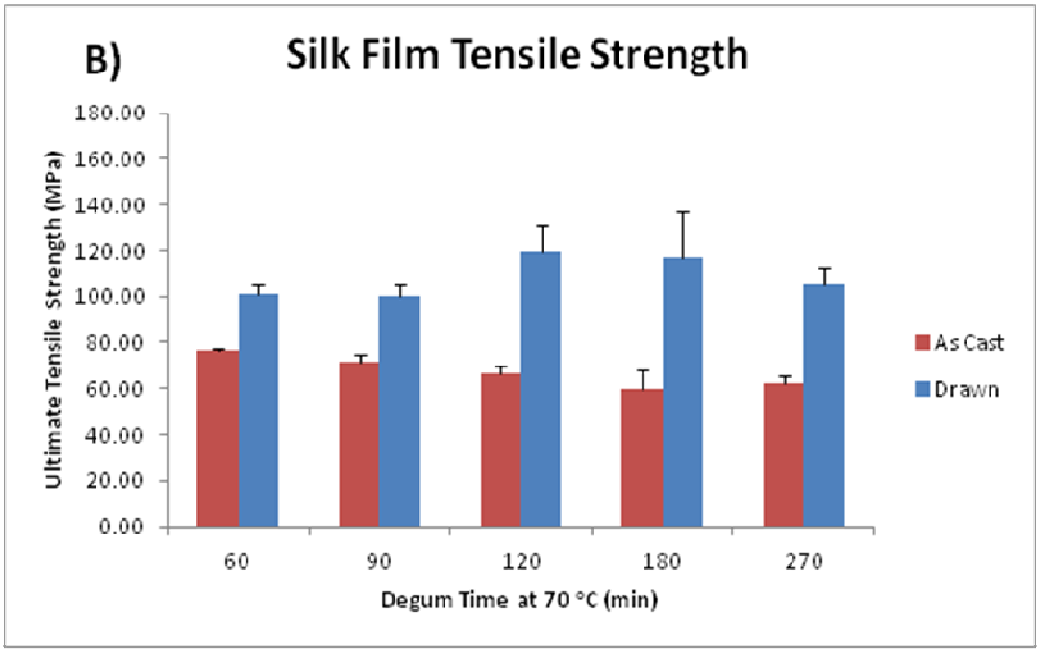

Figure 27 - Ultimate tensile strength of silk films in as cast and steam drawn states. (A) Films of different degum times at boiling temperature. (B) Films of different degum times at 70 °C.

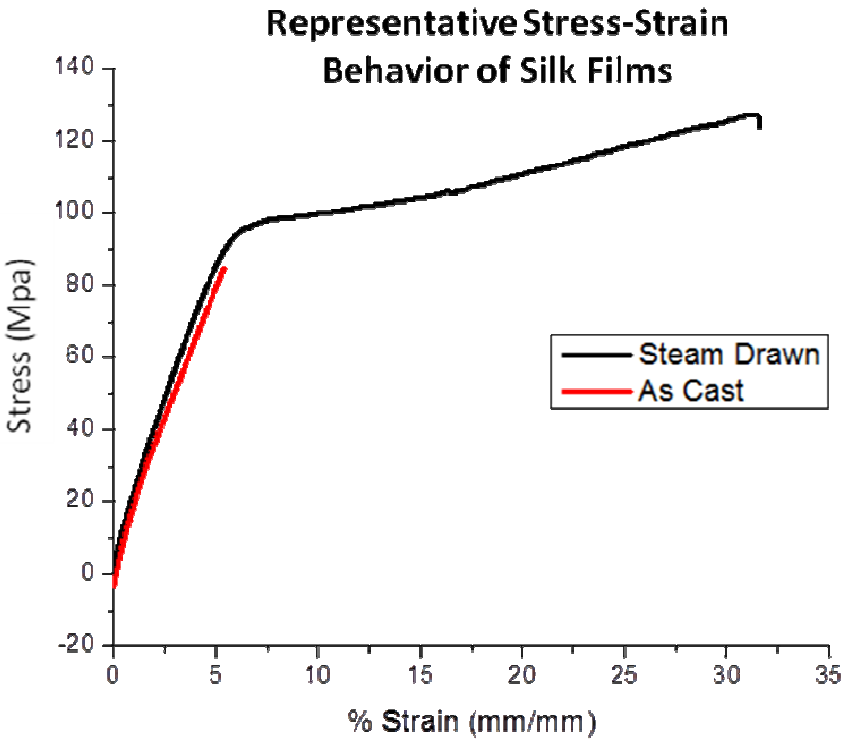

Figure 28 - Representative material behavior of as cast and steam drawn silk films. As cast film shows brittle behavior while steam drawn exhibits significantly enhanced ductility.

Table 5 - Tabulated mechanical data for as cast and steam drawn films for boiled and 70 °C degummed samples.

	As Cast Modulus (GPa)	Steam Drawn Modulus (GPa)	As Cast Extensibility (%)	Steam Drawn Extensibility (%)	As Cast Tensile Strength (MPa)	Steam Drawn Tensile Strength (MPa)
5mb	1.5 +/- 0.1	1.9 +/- 0.1	5.3 +/- 0.4	23.4 +/- 5.8	83.3 +/- 7.5	122.8 +/- 13.4
10mb	1.3 +/- 0.2	1.9 +/- 0.2	7.2 +/- 0.8	20.0 +/- 2.8	86.5 +/- 6.1	122.5 +/- 11.2
15mb	1.0 +/- 0.1	1.8 +/- 0.2	7.8 +/- 1.2	44.9 +/- 13.1	74.3 +/- 2.7	142.5 +/- 15.2
20mb	1.1 +/- 0.1	2.4 +/- 0.2	7.1 +/- 0.4	23.7 +/- 5.8	79.1 +/- 4.0	121.0 +/- 14.9
30mb	1.3 +/- 0.1	1.8 +/- 0.0	6.8 +/- 0.3	23.8 +/- 7.2	84.7 +/- 7.4	98.0 +/- 6.6
60mb	1.3 +/- 0.1	1.8 +/- 0.2	5.4 +/- 0.5	5.1 +/- 1.3	74.3 +/- 5.5	75.5 +/- 11.2
70C-60m	1.8 +/- 0.1	2.1 +/- 0.2	4.1 +/- 0.3	20.2 +/- 4.5	76.3 +/- 1.2	101.0 +/- 3.9
70C-90m	2.0 +/- 0.1	2.0 +/- 0.1	3.4 +/- 0.3	21.4 +/- 4.5	71.7 +/- 3.5	100.3 +/- 5.0
70C-120m	1.3 +/- 0.0	2.1 +/- 0.1	5.0 +/- 0.2	35.4 +/- 12.0	66.5 +/- 3.6	119.9 +/- 11.6
70C-180m	1.0 +/- 0.1	2.2 +/- 0.2	5.3 +/- 0.7	19.7 +/- 7.2	59.9 +/- 8.8	117.4 +/- 20.0
70C-270m	1.1 +/- 0.1	2.0 +/- 0.1	5.0 +/- 0.5	15.6 +/- 9.5	61.9 +/- 4.0	105.4 +/- 7.3

4.2.3. FTIR Spectra

Comparison of the FTIR spectra of films cast from differently degummed solutions did not reveal any between group differences in the as cast, post-treated, or steam drawn conditions as shown in Figures 29, 30 and 31 respectively. As cast samples all exhibited a primarily silk I conformation with a broad peak between 1650 and 1630 cm^{-1}. The conformational response to post-treatment was similarly not influenced by the molecular weight distribution of the fibroin. The spectral shifts toward 1620 cm^{-1} exhibited in 5mb, 30mb (not shown) and 60mb were characteristic of the transition to β-sheet in response to methanol treatment and water annealing. However, there were no differences in the response between experimental conditions. Additionally, the spectral shifts exhibited due to steam drawing did not indicate differences in conformation between the groups.

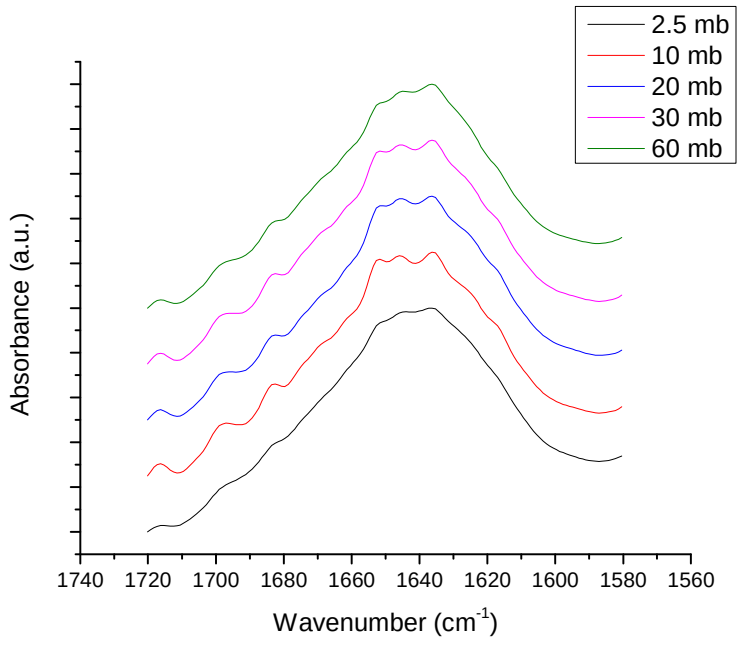

Figure 29 - Amide I band of FTIR spectra of different silk films cast from differently degummed solutions. Degum time does not result in detectable conformation differences in silk films.

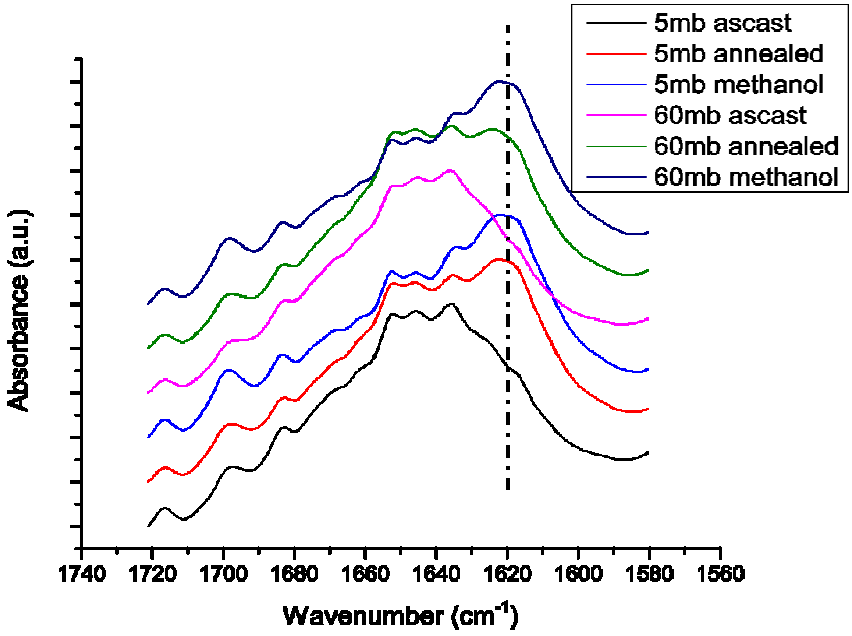

Figure 30 - Amide I band of FTIR spectra of 5mb and 60mb cast films subjected to water annealing and methanol treatments. Spectra show characteristic shift to β-sheet (vertical line at 1620 cm^{-1}) with post-treatment, but inter-group differences are not apparent.

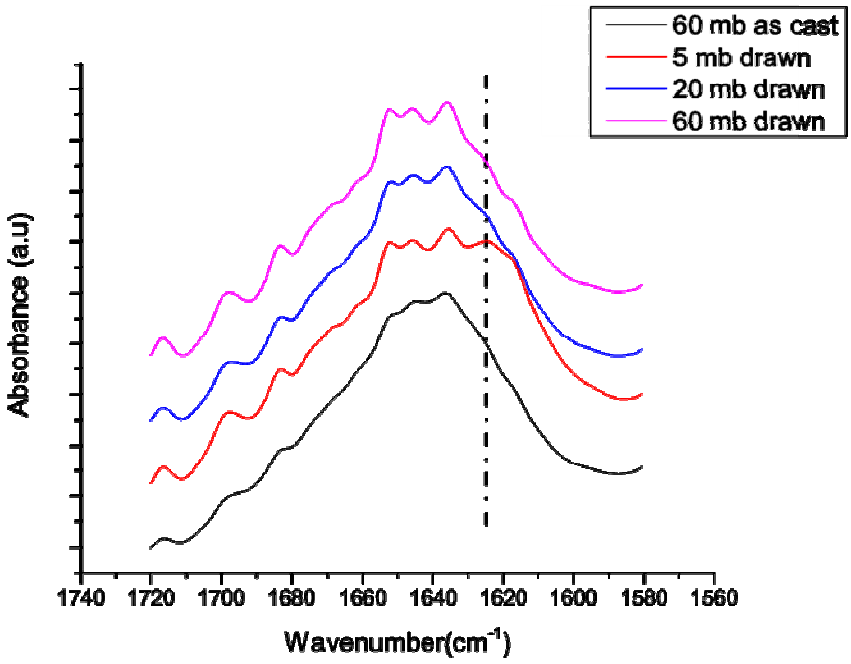

Figure 31 - Amide I band of FTIR spectra of silk films cast from differently degummed solutions and steam drawn. Only the 5mb spectra show shift toward β-sheet while 20mb and 60mb samples exhibit behavior similar to the as cast condition. 60mb as-cast film included for comparison.

4.3. Discussion

While gentle degumming conditions were able to generate silk solutions with similar rheological properties to native dope, they were unable to generate films to match the robust mechanical properties of the silk fibers. As depicted in Figure 32, the best steam stretched films were able to roughly match the modulus and extensibility of native fibers, however, the breaking strength of the films was below 30% of the strength of fibers. In addition the FTIR spectra of films from differently degummed silks respond similarly to post treatment steps, indicating that degumming does not significantly affect the conformation of the proteins.

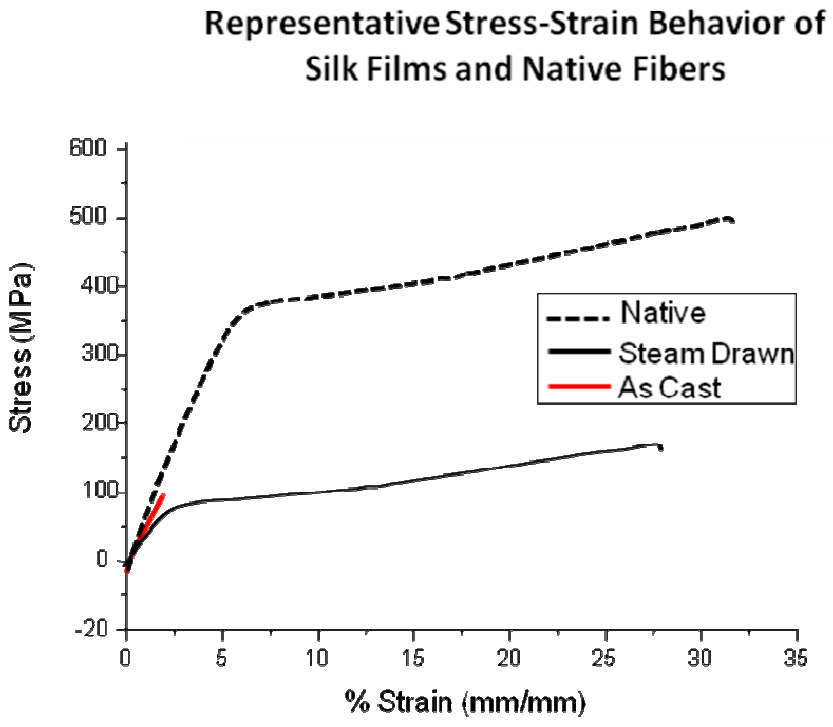

Figure 32 - Schematic representation of stress-strain response of native fibers, steam drawn silk films and as cast films.

Despite the lack of a significant increase of material properties with less aggressive degumming, several trends emerged that suggest avenues for further work to optimize regenerated silk properties. First, a relationship between degumming time, as cast modulus, drawn extensibility and drawn tensile strength was observed. Second, steam drawing resulted in increases in all mechanical properties measured; elastic modulus, extensibility and ultimate tensile strength.

As seen in Figures 25-27, the 15mb degumming condition exhibited the highest extensibility and tensile strength after steam drawing, while having the lowest as cast elastic modulus. This indicates that the 15mb group provides the optimal combination of fully disrupting molecular associations while minimizing degradation of the component proteins. These properties may also be the result of film casting within 10 days of solution production. Zainuddin, et al. showed that the rheology of 60mb solutions showed an inversion from a gel to liquid-like state and significant decrease in viscosity within the first month after production. It is likely that these transition and aggregation kinetics are dependent on the state of protein degradation. Therefore it is plausible that the 15mb solutions reached their optimal self-assembly stage in the +/- 10 days of storage at 4 ^{o}C following generation of the solution.

Additionally, the atypical behavior where modulus, extensibility and tensile strength all increased with steam drawing, supported by Yin, et al.'s work [45], implies that controlled drawing under plasticized conditions may allow tuning of the mechanical properties. In most engineering materials, improvement in one property is usually to the detriment of others, which does not occur with

the silk fibroin films. While there are surely limits to this behavior, at lower levels of strain this is highly advantageous and can likely be exploited to optimize material properties for specific applications. Zhou et al. probably explored this specific phenomenon in their regenerated fibers extruded and drawn in ammonium sulfate. They showed that draw ratios up to four times the original length caused increase in all material properties; however, at a draw ratio of six, tensile strength was increased, while extensibility was decreased. This suggests an optimum draw ratio of approximately 4 times the original length, which is roughly the drawing limit encountered during the drawing of cast films in steam.

4.3.1. Optimized Mechanical Properties

Based on the experimental conditions tested and reported here, there are a number of recommendations for producing regenerated silks with enhanced mechanical properties. The optimal degumming condition appears to be boiling for 15 minutes in a 0.02 M solution of Na_2CO_3, with standard rinsing, dissolving and dialysis protocols. Following removal of the solution from dialysis cassettes it should be centrifuged and allowed to age at 4 ^{o}C for approximately 7-10 days. After proper aging, the solution should be cast into a film or extruded into a fiber and allowed to slowly dry and self assemble. Once all water has evaporated the film or fiber should be drawn over steam to the maximum extent practicable. This procedure has been shown to produce significantly stronger and more ductile ($p < 0.01$) silks than other conditions.

5. Mechanism and Kinetics of Self Assembly

While optimizing the specific parameters to maximize mechanical properties is an important step, an effort was also undertaken to understand the underlying mechanisms and kinetics of silk fibroin self assembly. A review of current literature in combination with the data presented here provides some potential insight into why regenerated silks do not perform as well mechanically as native fibers.

Recently, Lu, et al. has shown that slow drying and concentration of regenerated silk solution at room temperature results in aggregation of the fibroin chains into micelles, with further rearrangement into nanofilaments and crystallation as time elapses. For a 20mb solution they claim that this self assembly process takes approximately one week, but these kinetics can be modulated by varying the drying rate [76]. Figure 33 shows a schematic of Lu, et al.'s proposed mechanism of self assembly, where hydrophobic blocks (yellow) are sequestered inside a shell of hydrophilic terminals and linkers (green and blue). As the assembly process progresses, residual water inside the micelle, denoted as green circle at the center, is forced out and the micelle becomes more compact going from 20 - 200 nm in diameter to 10 – 100 nm. Self assembly is completed when all water is removed and crystallization occurs.

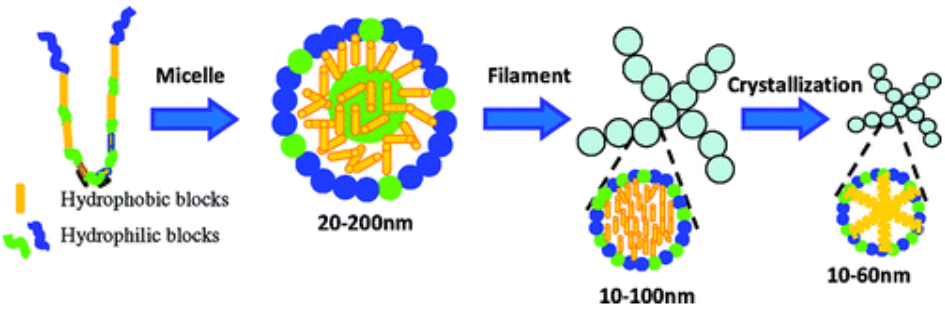

Figure 33 - Self-ssembly model including micelle formation, further rearrangement of micelles, nanofilament formation, and crystallization of silk fibroin. From Lu, et al. 2012 [76].

Holland, et al. have also proposed a novel assembly mechanism, referring to it as an "aquamelts" and describing it as a subclass of polymers. They suggest that shear is a required component of the self assembly mechanism and is what induces assembly of the polymers. The mechanism was developed using silk fibroin extracted from the silkworm that was simultaneously sheared and imaged using polarized light [77]. Due to their use of highly concentrated, native dope, it is likely that some of the aggregation, micelle and nanofilament formation as posited by Lu, et al. [76] had already occurred. This mechanism is likely to explain in part the changes that occur when silk films are drawn in the presence of a plasticizing agent such as water or steam.

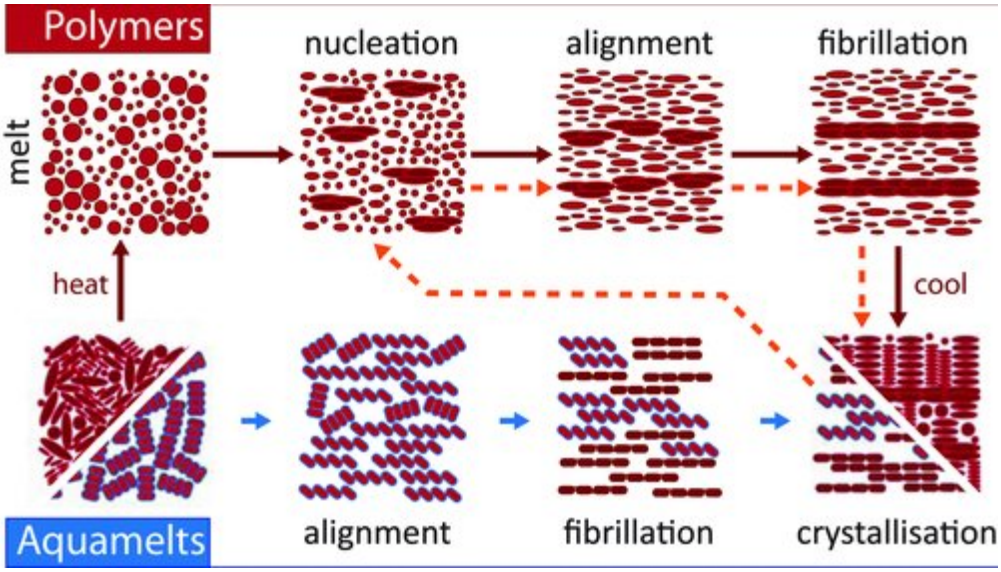

Figure 34 - Proposed mechanism of silk fiber formation as an aquamelt (blue arrows) and its relation to polymer melts (red arrows). Horizontal arrows depict shearing, with length corresponding to energy input required for fibrillation. From Holland, et al. 2012 [77].

While these proposed mechanisms are likely accurate for native silk fibroin, they are not as well defined for regenerated solutions. Specifically, the mechanisms presuppose the existence of highly hydrophilic N and C terminals as shown by Jin and Kaplan [49]. Based on the pattern of degradation exhibited in the SDS-PAGE gels, it is likely that one or both of these hydrophilic ends are cleaved during the regeneration process. Thus, while the hydrophilic linkers may serve as surrogate terminals, the degree of association and packing of degraded fibroin micelles and nanofilaments are unlikely to be as strong as those of native proteins. Based on these observations, proposed modified versions of Lu, et al.'s mechanisms and kinetics are presented in Figure 35. Proposed mechanisms are provided for three types of regenerated solutions, gently degummed (2.5mb or 5mb), standard degumming (15mb or 20mb) and aggressively degummed (60+mb).

For the gently degummed solutions, we suggest that the hydrophilic N and C terminals are largely intact and the fresh solution is close to native in both behavior and make-up. The difference between these regenerated solutions and native is the existence of residual entanglements that were not completely removed during degumming and solvation. Thus, even though the individual protein strands have their native hydrophilic-hydrophobic-hydrophilic tri-block structure, they are prevented from properly folding and assembling into micelles. As the drying and concentration processes progress, the incompletely formed micelles, condense into nanofilaments and crystallize in place. When these structures are subject to shear they initially behave as fully formed micelles, however, as strain is increased, the residual entanglements are engaged, limiting the extensional flow of the molecules. This inhibition of molecular movement then results in stiffening and failure of the material. As the orientation of these entanglements may be off the axis of drawing, both the tensile strength and elasticity of the sample are degraded.

In optimized or standard degumming solutions, a significant number of the N or C terminals have been cleaved during reconstitution, resulting in a number of linker sequences serving as defacto hydrophilic terminals. However, unlike the gently degummed solutions, residual entanglements are substantially broken. As the linker sequences are not as highly hydrophilic as the N or C terminals the micelle formation is retarded as the propensity for the hydrophilic ends to shield the hydrophobic interior is lessened. From this point, self assembly progresses as for native fibroin. When these micelles are subject to shear forces they readily

flow and elongate as proposed by Jin and Kaplan [49]. However, due to the fact that they are more loosely associated, they are able to undergo a greater degree of elongation, but are unable to completely engage reducing the tensile strength as compared to native silks.

When degumming times are increased beyond the 15 to 20 minute time frame, significant degradation of the protein chain is experienced. All of the hydrophilic terminals are lost and the linkers are forced serve as the hydrophilic outer layer during micelle formation. The result is a weakly formed micelle that lacks the highly ordered and layered architecture of native silks. When these materials are sheared the lack of interfacial association between hydrophilic outer layers limits tensile strength, while shortened chain lengths inhibit extensibility.

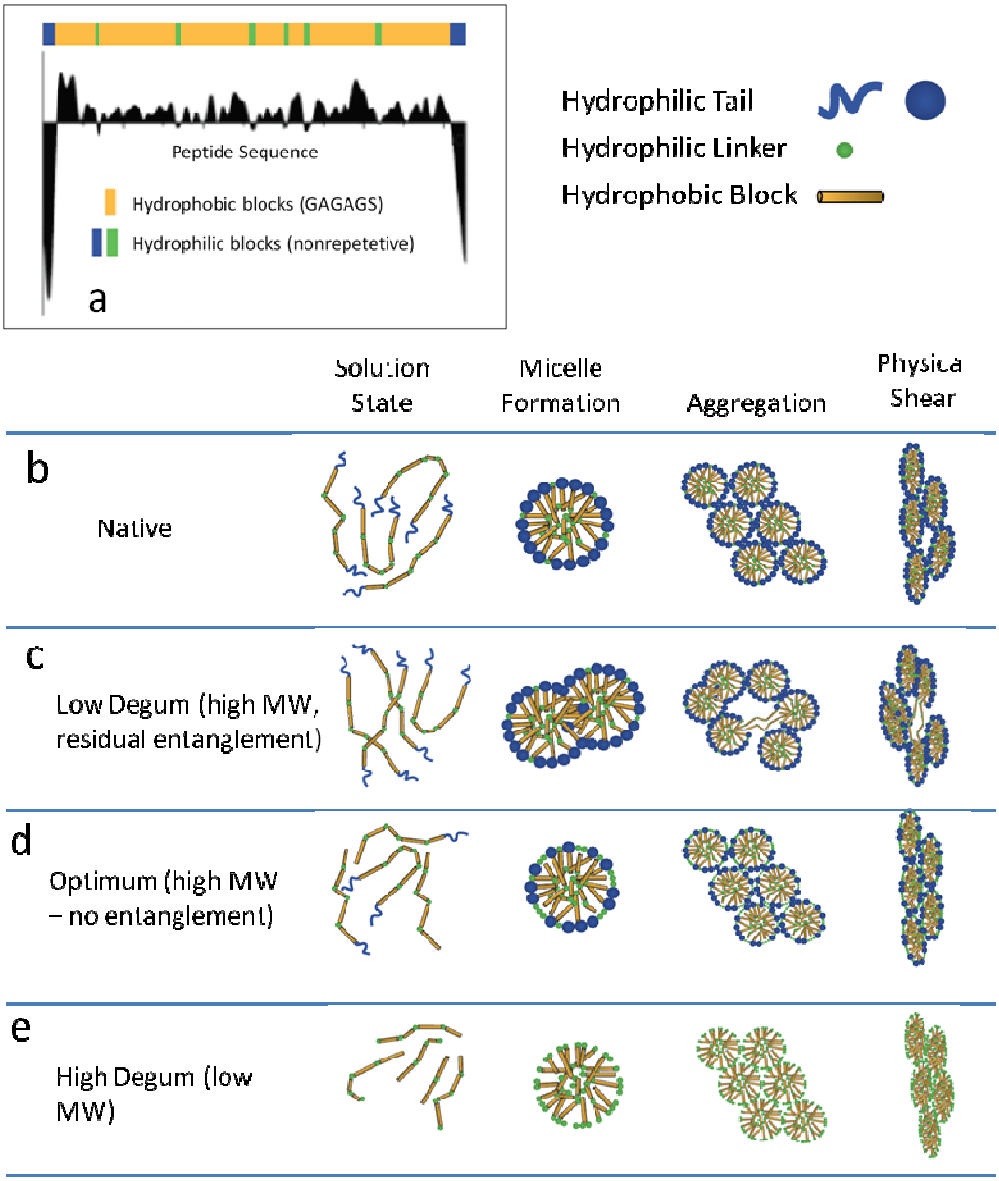

Figure 35 - Proposed mechanisms of self assembly for differently degummed silk solutions. (a) Hydrophobicity pattern in fibroin chain [49] (b) Mechanism of self assembly for native silks by Jin and Kaplan. Protein chains assemble into micelles, for globules and are sheared to produce fibers [49]. (c) Gently degummed silks retain residual entanglements which inhibit micelle and globule formation, and prevent efficient extensional shear. (d) Optimally degummed silks have all residual entanglements removed, but have shortened chain lengths and fewer hydrophilic tails. This allows native like micelle and globule formation but weaker inter-micelle hydrophilic associations allowing excellent extensional flow, but lower tensile strength. (D) Aggressively degummed silks with shorter chain lengths and no remaining hydrophilic tails. Micelle formation and globule formation occur, but have ineffective shielding of the hydrophobic core. Short chain length and weak micelle associations limit both extensibility and strength.

6. Conclusion

A review of all the data suggests that the mechanisms involved in silk assembly are more nuanced than expected. For semi-crystalline synthetic polymers there are well established relationships between molecular weight, polydispersity index (PDI) and mechanical properties [78, 79]. However, this direct relationship does not hold for fibroin proteins, where increased molecular weight and decreased PDI actually result in lower strength and ductility following drawing. Instead of a direct correlation, an optimal degumming time (molecular weight, PDI) was found to occur in the 15mb group. It is proposed that this optimal degumming condition is the result of a complete removal of residual molecular entanglements, while minimizing core degradation. A summary of major conclusions is included in Table 6.

Table 6 - Summary of conclusions.

1.	Regenerated silk solutions are fundamentally different than native silk dopes.
2.	Low degumming times/temperatures fail to fully disrupt all molecular associations.
3.	Optimal degumming in boiling Na_2CO_3 is approx. 15 min.
4.	Aggregation of protein chains into micelles over time is critical.
5.	In-situ or post drawing is required for molecular alignment.

References

1. Altman, G.H., et al., *Silk-based biomaterials.* Biomaterials, 2003. **24**(3): p. 401-416.

2. Wang, Y., et al., *Stem cell-based tissue engineering with silk biomaterials.* Biomaterials, 2006. **27**(36): p. 6064-6082.

3. Inouye, K., et al., *Use of Bombyx mori silk fibroin as a substratum for cultivation of animal cells.* Journal of Biochemical and Biophysical Methods, 1998. **37**(3): p. 159-164.

4. Cannon, G.M., et al., *Silk as a Novel Biomaterial in Bladder Tissue Engineering.* Journal of Pediatric Urology, 2010. **6**: p. S82.

5. Wenk, E., et al., *Silk fibroin spheres as a platform for controlled drug delivery.* Journal of Controlled Release, 2008. **132**(1): p. 26-34.

6. Meinel, L. and D.L. Kaplan, *Silk constructs for delivery of muskuloskeletal therapeutics.* Advanced drug delivery reviews, 2012.

7. Hofmann, S., et al., *Silk fibroin as an organic polymer for controlled drug delivery.* Journal of Controlled Release, 2006. **111**(1): p. 219-227.

8. Omenetto, F.G. and D.L. Kaplan, *New opportunities for an ancient material.* Science, 2010. **329**(5991): p. 528-531.

9. Demura, M. and T. Asakura, *Immobilization of glucose oxidase with Bombyx mori silk fibroin by only stretching treatment and its application to glucose sensor.* Biotechnology and Bioengineering, 1989. **33**(5): p. 598-603.

10. Amsden, J.J., et al. *Silk fibroin biosensor based on imprinted periodic nanostructures*. 2009. IEEE.

11. Mita, K., S. Ichimura, and T.C. James, *Highly repetitive structure and its organization of the silk fibroin gene.* Journal of molecular evolution, 1994. **38**(6): p. 583-592.

12. Fu, C., Z. Shao, and V. Fritz, *Animal silks: their structures, properties and artificial production.* Chemical Communications, 2009(43): p. 6515-6529.

13. Vepari, C. and D.L. Kaplan, *Silk as a biomaterial.* Progress in Polymer Science, 2007. **32**(8-9): p. 991-1007.

14. Sugihara, A., et al., *Promotive effects of a silk film on epidermal recovery from full-thickness skin wounds (44552).* Experimental Biology and Medicine, 2000. **225**(1): p. 58-64.

15. Yeo, J.H., et al., *The effects of PVA/Chitosan/Fibroin (PCF)-blended spongy sheets on wound healing in rats.* Biological and Pharmaceutical Bulletin, 2000. **23**(10): p. 1220-1223.

16. Meinel, L., et al., *Bone tissue engineering using human mesenchymal stem cells: Effects of scaffold material and medium flow.* Annals of Biomedical Engineering, 2004. **32**(1): p. 112-122.

17. Meinel, L., et al., *Silk implants for the healing of critical size bone defects.* Bone, 2005. **37**(5): p. 688-698.

18. Kim, H.J., et al., *Influence of macroporous protein scaffolds on bone tissue engineering from bone marrow stem cells.* Biomaterials, 2005. **26**(21): p. 4442-4452.

19. Meinel, L., et al., *Silk based biomaterials to heal critical sized femur defects.* Bone, 2006. **39**(4): p. 922-931.

20. Meinel, L., et al., *Osteogenesis by human mesenchymal stem cells cultured on silk biomaterials: Comparison of adenovirus mediated gene transfer and protein delivery of BMP-2.* Biomaterials, 2006. **27**(28): p. 4993-5002.

21. Karageorgiou, V., et al., *Porous silk fibroin 3-D scaffolds for delivery of bone morphogenetic protein-2 in vitro and in vivo.* Journal of Biomedical Materials Research - Part A, 2006. **78**(2): p. 324-334.

22. Marolt, D., et al., *Bone and cartilage tissue constructs grown using human bone marrow stromal cells, silk scaffolds and rotating bioreactors.* Biomaterials, 2006. **27**(36): p. 6138-6149.

23. Karageorgiou, V., et al., *Bone morphogenetic protein-2 decorated silk fibroin films induce osteogenic differentiation of human bone marrow stromal cells.* Journal of Biomedical Materials Research - Part A, 2004. **71**(3): p. 528-537.

24. Sofia, S., et al., *Functionalized silk-based biomaterials for bone formation.* Journal of Biomedical Materials Research, 2001. **54**(1): p. 139-148.

25. Kino, R., et al., *Deposition of bone-like apatite on modified silk fibroin films from simulated body fluid.* Journal of Applied Polymer Science, 2006. **99**(5): p. 2822-2830.

26. Motta, A., et al., *Fibroin hydrogels for biomedical applications: Preparation, characterization and in vitro cell culture studies.* Journal of Biomaterials Science, Polymer Edition, 2004. **15**(7): p. 851-864.

27. Fini, M., et al., *The healing of confined critical size cancellous defects in the presence of silk fibroin hydrogel.* Biomaterials, 2005. **26**(17): p. 3527-3536.

28. Li, C., et al., *Electrospun silk-BMP-2 scaffolds for bone tissue engineering.* Biomaterials, 2006. **27**(16): p. 3115-3124.

29. Kim, K.H., et al., *Biological efficacy of silk fibroin nanofiber membranes for guided bone regeneration.* Journal of Biotechnology, 2005. **120**(3): p. 327-339.

30. Meinel, L., et al., *Engineering cartilage-like tissue using human mesenchymal stem cells and silk protein scaffolds.* Biotechnology and Bioengineering, 2004. **88**(3): p. 379-391.

31. Wang, Y., et al., *Cartilage tissue engineering with silk scaffolds and human articular chondrocytes.* Biomaterials, 2006. **27**(25): p. 4434-4442.

32. Morita, Y., et al., *Visco-elastic properties of cartilage tissue regenerated with fibroin sponge.* Bio-Medical Materials and Engineering, 2002. **12**(3): p. 291-298.

33. Morita, Y., et al., *Frictional properties of regenerated cartilage in vitro.* Journal of Biomechanics, 2006. **39**(1): p. 103-109.

34. Aoki, H., et al., *Culture of chondrocytes in fibroin-hydrogel sponge.* Bio-Medical Materials and Engineering, 2003. **13**(4): p. 309-316.

35. Chen, J., et al., *Human bone marrow stromal cell and ligament fibroblast responses on RGD-modified silk fibers.* Journal of Biomedical Materials Research - Part A, 2003. **67**(2): p. 559-570.

36. Altman, G.H., et al., *Silk matrix for tissue engineered anterior cruciate ligaments.* Biomaterials, 2002. **23**(20): p. 4131-4141.

37. Moreau, J.E., et al., *Sequential growth factor application in bone marrow stromal cell ligament engineering.* Tissue Engineering, 2005. **11**(11-12): p. 1887-1897.

38. Kardestuncer, T., et al., *RGD-tethered silk substrate stimulates the differentiation of human tendon cells.* Clinical Orthopaedics and Related Research, 2006(448): p. 234-239.

39. Hu, K., et al., *Biocompatible fibroin blended films with recombinant human-like collagen for hepatic tissue engineering.* Journal of bioactive and compatible polymers, 2006. **21**(1): p. 23-37.

40. Dal Pra, I., et al., *De novo engineering of reticular connective tissue in vivo by silk fibroin nonwoven materials.* Biomaterials, 2005. **26**(14): p. 1987-1999.

41. Unger, R.E., et al., *Endothelialization of a non-woven silk fibroin net for use in tissue engineering: Growth and gene regulation of human endothelial cells.* Biomaterials, 2004. **25**(21): p. 5137-5146.

42. Fuchs, S., et al., *Outgrowth endothelial cells isolated and expanded from human peripheral blood progenitor cells as a potential source of autologous cells for endothelialization of silk fibroin biomaterials.* Biomaterials, 2006. **27**(31): p. 5399-5408.

43. Lee, K.Y., et al., *Effect of surface properties on the antithrombogenicity of silk fibroin/S-carboxymethyl kerateine blend films.* Journal of Biomaterials Science, Polymer Edition, 1998. **9**(9): p. 905-914.

44. Holland, C., et al., *Natural and unnatural silks.* Polymer, 2007. **48**(12): p. 3388-3392.

45. Yin, J., et al., *Enhancing the Toughness of Regenerated Silk Fibroin Film through Uniaxial Extension.* Biomacromolecules, 2010. **11**(11): p. 2890-2895.

46. Lee, Y.W., *Silk reeling and testing manual*. Vol. 136. 1999: Food & Agriculture Organization of the UN (FAO).

47. Zhou, C.Z., et al., *Silk fibroin: structural implications of a remarkable amino acid sequence.* Proteins: Structure, Function, and Bioinformatics, 2001. **44**(2): p. 119-122.

48. Murphy, A.R. and D.L. Kaplan, *Biomedical applications of chemically-modified silk fibroin.* Journal of Materials Chemistry, 2009. **19**(36): p. 6443-6450.

49. Jin, H.J. and D.L. Kaplan, *Mechanism of silk processing in insects and spiders.* Nature, 2003. **424**(6952): p. 1057-1061.

50. Holland, C., et al., *Polymer Fibers: Silk and Synthetic Polymers: Reconciling 100 Degrees of Separation (Adv. Mater. 1/2012).* Advanced Materials, 2012. **24**(1): p. 104-104.

51. Takei, F., et al., *Further evidence for importance of the subunit combination of silk fibroin in its efficient secretion from the posterior silk gland cells.* The Journal of cell biology, 1987. **105**(1): p. 175-180.

52. Tanaka, K., K. Mori, and S. Mizuno, *Immunological identification of the major disulfide-linked light component of silk fibroin.* Journal of biochemistry, 1993. **114**(1): p. 1-4.

53. Tanaka, K., et al., *Determination of the site of disulfide linkage between heavy and light chains of silk fibroin produced by Bombyx mori.* Biochimica et Biophysica Acta (BBA)-Protein Structure and Molecular Enzymology, 1999. **1432**(1): p. 92-103.

54. Takasu, Y., H. Yamada, and K. Tsubouchi, *Isolation of Three Main Sericin Components from the Cocoon of the Silkworm, Bombyx mori.* Bioscience, Biotechnology, and Biochemistry, 2002. **66**(12): p. 2715-2718.

55. Rockwood, D.N., et al., *Materials fabrication from Bombyx mori silk fibroin.* Nat. Protocols, 2011. **6**(10): p. 1612-1631.

56. Panilaitis, B., et al., *Macrophage responses to silk.* Biomaterials, 2003. **24**(18): p. 3079-3085.

57. Altman, G.H.C., Jingsong; Horan, Rebecca; Horan, David, *Immunoneutral Silk-Fiber-Based Medical Devices*, 2004, Tissue Regeneration, Inc.: United States. p. 45.

58. Yamada, H., et al., *Preparation of undegraded native molecular fibroin solution from silkworm cocoons.* Materials Science and Engineering: C, 2001. **14**(1-2): p. 41-46.

59. Jiang, P., et al., *Tensile behavior and morphology of differently degummed silkworm (Bombyx mori) cocoon silk fibres.* Materials Letters, 2006. **60**(7): p. 919-925.

60. Zhao, H.P., X.Q. Feng, and H.J. Shi, *Variability in mechanical properties of< i> Bombyx mori</i> silk.* Materials Science and Engineering: C, 2007. **27**(4): p. 675-683.

61. Freddi, G., R. Mossotti, and R. Innocenti, *Degumming of silk fabric with several proteases.* Journal of Biotechnology, 2003. **106**(1): p. 101-112.

62. Ho, M., H. Wang, and K. Lau, *Effect of degumming time on silkworm silk fibre for biodegradable polymer composites.* Applied Surface Science, 2012. **258**(8): p. 3948-3955.

63. Wray, L.S., et al., *Effect of processing on silk-based biomaterials: Reproducibility and biocompatibility.* Journal of Biomedical Materials Research Part B: Applied Biomaterials, 2011. **99B**(1): p. 89-101.

64. Zhang, c., et al., *Flexibility regeneration of silk fibroin in vitro.* Biomacromolecules, 2012.

65. Zhou, G., et al., *Silk Fibers Extruded Artificially from Aqueous Solutions of Regenerated Bombyx mori Silk Fibroin are Tougher than their Natural Counterparts.* Advanced Materials, 2009. **21**(3): p. 366-370.

66. Wei, W., et al., *Bio-inspired capillary dry spinning of regenerated silk fibroin aqueous solution.* Materials Science and Engineering: C, 2011. **31**(7): p. 1602-1608.

67. Kinahan, M.E., et al., *Tunable Silk: Using Microfluidics to Fabricate Silk Fibers with Controllable Properties.* Biomacromolecules, 2011. **12**(5): p. 1504-1511.

68. Marsano, E., et al., *Wet spinning of Bombyx mori silk fibroin dissolved in N-methyl morpholine N-oxide and properties of regenerated fibres.* International Journal of Biological Macromolecules, 2005. **37**(4): p. 179-188.

69. Phillips, D.M., et al., *Regenerated silk fiber wet spinning from an ionic liquid solution.* Journal of Materials Chemistry, 2005. **15**(39): p. 4206-4208.

70. Yan, J., et al., *Wet-Spinning of Regenerated Silk Fiber from Aqueous Silk Fibroin Solution: Discussion of Spinning Parameters.* Biomacromolecules, 2009. **11**(1): p. 1-5.

71. Teh, T.K.H. and et al., *Optimization of the silk scaffold sericin removal process for retention of silk fibroin protein structure and mechanical properties.* Biomedical Materials, 2010. **5**(3): p. 035008.

72. Sasaki, T. and H. Noda, *Studies on silk fibroin of Bombyx mori directly extracted from the silk gland: I. Molecular weight determination in guanidine hydrochloride or urea solutions.* Biochimica et Biophysica Acta (BBA) - Protein Structure, 1973. **310**(1): p. 76-90.

73. Weber, K. and M. Osborn, *The reliability of molecular weight determinations by dodecyl sulfate-polyacrylamide gel electrophoresis.* Journal of Biological Chemistry, 1969. **244**(16): p. 4406-4412.

74. Zainuddin, T.T., et al., *The behavior of aged regenerated< i> Bombyx mori</i> silk fibroin solutions studied by< sup> 1</sup> H NMR and rheology.* Biomaterials, 2008. **29**(32): p. 4268-4274.

75. Lu, Q., et al., *Water-insoluble silk films with silk I structure.* Acta Biomaterialia, 2010. **6**(4): p. 1380-1387.

76. Lu, Q., et al., *Silk Self-Assembly Mechanisms and Control-From Thermodynamics to Kinetics.* Biomacromolecules, 2012.

77. Holland, C., et al., *Silk and Synthetic Polymers: Reconciling 100 Degrees of Separation.* Advanced Materials, 2012.

78. Hallam, M., G. Pollard, and I. Ward, *Relationship between tensile strength and molecular weight of highly drawn polyethylenes.* Journal of materials science letters, 1987. **6**(8): p. 975-976.

79. Hallam, M., et al., *A study of the effect of molecular weight on the tensile strength of ultra-high modulus polyethylenes.* Journal of materials science, 1986. **21**(12): p. 4199-4205.